2.1. INTRODUCTION

Nowadays, nanobased research is a potent field of attention because NPs has a variety of unique applications compare to their bulk counterpart. Recently, the NMNPs like silver, palladium, gold etc., has been prime attention for practical applications and also due to their chemical [Marbella *et al*., (2015); Linic *et al*., (2015)], electrical [Benson *et al*., (2015)], optical [Lin *et al*., (2011); Wu *et al*., (2014)] and electrocatalytic properties [Xu *et al*., (2015); Jeong *et al*., (2015); Deogratias *et al*., (2015)]. Out of these NMNPs, AgNPs is of immense interest due to their unique applications such as antimicrobial agent [Panacek *et al*., (2006); Niu *et al*., (2012); Eckhardt *et al*., (2013); Rizzello *et al*., (2014)], catalysis [Santos *et al*., (2012); Neumann *et al*., (2013)], and printed electronics [Li *et al*., (2005); Lee *et al*., (2006); Shen *et al*., (2014)]. Inspired this notion, a variety of experimental techniques for synthesis of AgNPs has been reported. Various approaches has been invented to synthesized the AgNPs in which chemical and biological synthetic routes [Prasad *et al*., (2005); Chen *et al*., (2008); Li *et al*., (2010); Zhang *et al*., (2011); He *et al*., (2014)] has also been incorporated to enhance the performance of nanoparticles displaying improved properties with the aim to have a better control over the particle size, distribution and morphology. Chemical synthetic protocol is most frequently applied method for the preparation of AgNPs because, its need to a stable, colloidal dispersions in appropriate solvents (water or organic solvents) [Tao *et al*., (2006); Willy *et al*., 2005]. Various reducing agents like borohydride [Polte *et al*., (2012)], citrate [Wang and Ni., (2014)], ascorbate [Singha *et al*., (2014)], PVP [Pal *et al*., 2009] and elemental hydrogen [Lee *et al*., (2003); Ahmadi, *et al*., (2003)] have been used for the synthesis of AgNPs. However, the synthesis of stabilized functional AgNPs under ambient conditions remains a challenge [Sun and Xia., (2002); Li *et al*., (2005); Chernousova *et al*., (2013)] from following angles: (1) stability and dispersibility in a variety of solvents, (2) processability for nanocomposite formation (3) functional ability and biocompatibility for specific applications. The stabilization of AgNPs in different solvents is of paramount importance for their utilization as building blocks from both fundamental and applied considerations, since the AgNPs made through conventional chemical process are often soluble in either aqueous phase or in organic phase, limiting their role for practical applications. The synthesis of

AgNPs by chemical reduction methods is therefore often performed in the presence of various functionalized stabilizers in order to prevent unwanted agglomeration of the colloidal AgNPs. Accordingly there is a need of suitable reagents that not only acts as reducing agent but also efficiently stabilized the AgNPs. In this regard sol-gel processing offers a simple and versatile route to combine the favourable properties of functional alkoxysilanes having possibility for yielding organic, inorganic material with metal nanoparticles (MNPs).

Organically Functionalized alkoxysilane have shown potential applications in the development of nanostructured thin film as organically modified silicates (ORMOSIL) designing electrochemical sensors **[**Pandey *et al*., (1999a); Pandey *et al*., (1999b); Pandey *et al*., (1999c); Pandey *et al*., (1999d); Pandey *et al*., (1999e); Pandey *et al*., (1999f); Pandey *et al*., (2003a); Pandey *et al*., (2001d); Walcarius, (2013); Walcarius *et al*., (2005); Walcarius and Collinson, (2009)]. Additionally, functionalized alkoxysilanes have been used as stabilizers to complex metal ions in the sol form [Selvakannan *et al*., (2004); Bhargava *et al*., (2005); Ballarin *et al*., (2008)]. These alkoxysilanes under optimum ratio of hydrophilic and hydrophobic components like 3-APTMS, 2-(3, 4-epoxycyclohexyl) ethyltrimethoxysilane, TMS and GPTMS results into the formation of ORMOSIL having nanostructured domains [Pandey *et al*., (1999a); Pandey *et al*., (1999c); Pandey *et al*., (2001b)]. These ormosil films provided excellent matrix for the encapsulation of redox active proteins and biological sensing component which not only facilitate in probing biochemical interaction, but also introduced bioelectrocatalysis during electrochemical sensing. The major problem encountered during biochemical sensing while using such nanostructured matrix was poor diffusion of sensing reagent limiting the electrochemical sensing events together poor charge transport across the matrix. Subsequently, the diffusion limited conditions was controlled by incorporation of water leachable material and graphite particles [Tripathi., (2002)]. However, in order to facilitate the charge transfer process, attention on the incorporation of redox active materials along with redox biomolecules was attempted [Tripathi., (2002)]. Although, the stability of small redox molecule like Ferrocene within the nanostructured matrix

was exellent however, the encapsulated ferrocene was not efficient to communicate with this redox biomolecule due to restricted mobility of the same [Pandey *et al*., (2001c)]. Such problem directed to use electrocatalytic material within the nanostructured domain in order to overcome such limitation. Fortunately, the finding on the specific interaction of one of the alkoxysilane precursors like GPTMS and $PdCl_2$ has been recorded [Pandey *et al*., (2001c)]. It was found that $PdCl_2$ acting as a lewis acid opens the epoxide ring of GPTMS and inturn $PdCl_2$ was reduced. The reduced $PdCl_2$ was ultimately introduced within the nanostructured domain through sol-gel processing that introduced bioelectrocatalysis during biosensing. These findings demonstrated the reducing ability of GPTMS. Further, the use of 3-APTMS have shown potential activity as stabilizer of MNPs [Selvakannan *et al*., (2004); Bhargava *et al*., (2005);] serving as potential capping agent for metal cations. These finding directed us to investigate the reducing and stabilizing ability of GPTMS and 3-APTMS during the synthesis of AgNPs which is reported herein. The use of two alkoxysilanes may cause autohydrolysis, condensation and polycondensation leading to the formation of Si-O-Si linkage. Accordingly, attempts has been made to replace one of the alkoxysilanes by suitable organic reducing agents that not only enable the real synthesis of AgNPs in the presence of one of the alkoxysilane but also control the dispersibility of AgNPs in desired medium.

2.2. EXPERIMENTAL

2.2.1. Materials

3-Aminopropyltrimethoxysilane (3-APTMS), 3-Glycidoxypropyltrimethoxysilane (GPTMS) and $AgNO_3$ were obtained from Aldrich Chemical Co., India. Cyclohexanone, formaldehyde, methanol, butanol, acetonitrile, dichloromethane and toluene were purchased from Merck, India. All other chemicals employed were of analytical grade. Aqueous solutions were prepared by using doubly distilled-deionized water (Alga water purification system). Unless mentioned otherwise, all the experiments were performed at room temperature.

2.2.2. Preparation of Silver Nanoparticles (AgNPs)

2.2.2.1. Synthesis of AgNPs made through 3-APTMS and GPTMS mediated reaction

AgNPs was synthesized using $AgNO_3$, 3-APTMS and GPTMS was varied as presented in Table 2.1. Methanolic suspension of 3-APTMS treated Ag^+ ions was added to methanolic solution of GPTMS (Table 2.1). The resulting mixture was stirred over a vertex cyclo mixer for 2 min. The mixture was left to stand in the dark for 12 h. After this, the colour of the mixture turned to yellow indicating the formation of AgNPs. Different shades of AgNPs was prepared by varying the concentration of both 3-APTMS and GPTMS (Table 2.1., samples I, II, III……XX). The concentrations of 3-APTMS and GPTMS dependent formation of AgNPs were shown in term of "+" and "–" sign. An increase in number of "+" sign denotes an increase the rate of AgNPs formation by 20% whereas "–" sign represents that AgNPs are not formed under respective conditions (Table 2.1).

Table 2.1. The synthesis of AgNPs as a function of 3-APTMS and GPTMS concentrations containing $AgNO_3$ (0.025 M); "+" sign represents feasibility of AgNPs formation whereas "–" sign represents that AgNPs are not formed.

S. No	Sample Name	GPTMS (M)	3-APTMS (M)	AgNPs formation
1	I	4	0.05 ($AgNP_1$)	+++++
2	II	3	0.05	++++
3	V	4	0.1	++++
4	IX	4	0.5 ($AgNP_2$)	++++
5	III	2	0.05	+++
6	VI	3	0.1	+++
7	X	3	0.5	+++
8	XIII	4	1	+++
9	XVII	4	1.5	+++
10	IV	1	0.05	++
11	VII	2	0.1	++
12	XI	2	0.5 ($AgNP_3$)	++
13	XIV	3	1	++
14	XVIII	3	1.5	++
15	VIII	1	0.1	+
16	XII	1	0.5	+
17	XV	2	1	+
18	XVI	1	1	-
19	XIX	2	1.5	-
20	XX	1	1.5	-

2.2.2.2. Cyclohexanone and 3-APTMS mediated synthesis of AgNPs

A typical process for cyclohexanone and 3-APTMS mediated synthesis of AgNPs consisted of following steps: 50μL of 10 mM of $AgNO_3$ solution in methanol was premixed with 10μL of methanolic solution of 3-APTMS (0.25 M and 0.5 M) stirred for 2 min, followed by addition of cyclohexanone (1.9 M). The solution was kept undisturbed for 2 h. $AgNP_4$ and $AgNP_5$ of yellow colour were obtained within <3 h. The optimum concentrations of cyclohexanone/3-APTMS keeping constant concentrations of silver nitrate required for best AgNPs formation was achieved by varying the concentrations of one component while keeping fixed concentrations of second components as shown in Tables 2.2-3.

Table 2.2. Characteristics of different Silver nanoparticles (AgNPs) made from Cyclohexanone as a function of 3-APTMS concentration.

S. no.	$AgNO_3$ (M)	3-APTMS (M)	Cyclohexanone (M)	AgNPs formation	Extent of formation
a	0.01	$0.1x10^{-3}$	1.9	White	-
b	0.01	0.001	1.9	White	-
c	0.01	0.005	1.9	White	-
d	0.01	0.01	1.9	White	-
e	0.01	0.05	1.9	White	-
f	0.01	0.1	1.9	White	-
g	0.01	0.25	1.9	Light Yellow($AgNP_4$)	++
h	0.01	0.5	1.9	Yellow($AgNP_5$)	++++
i	0.01	1	1.9	Yellow	++++
j	0.01	2	1.9	Yellow	++++

Table 2.3. Characteristics of different Silver nanoparticles (AgNPs) as a function of Cyclohexanone concentration.

S. no.	$AgNO_3$ (M)	3-APTMS (M)	Cyclohexanone (M)	AgNPs formation	Extent of formation
i	0.01	0.5	0.3	White	-
ii	0.01	0.5	0.6	White	-
iii	0.01	0.5	0.9	Light Yellow	+
iv	0.01	0.5	1.4	Light Yellow	++
v	0.01	0.5	1.9	Dark Yellow	++++
vi	0.01	0.5	2.4	Light Yellow	+++
vii	0.01	0.5	2.8	Light Yellow	+++
viii	0.01	0.5	3.2	Light Yellow	+++
ix	0.01	0.5	3.5	Light Yellow	+++
x	0.01	0.5	3.8	Light Yellow	+++

2.2.2.3. Formaldehyde and 3-APTMS mediated synthesis of AgNPs

A typical process for formaldehyde and 3-APTMS mediated synthesis of AgNPs consisted of following steps: 50μL of 10 mM of $AgNO_3$ solution in methanol was premixed with 10μL of methanolic solution of desired concentrations of 3-APTMS stirred for 2 min, followed by addition of formaldehyde. The reaction mixture was turned into Dark yellow within 30 min. The optimum concentrations of formaldehyde/3-APTMS keeping constant concentrations of silver nitrate required for AgNPs formation was achieved by varying the concentrations of one component while keeping fixed concentrations of second components as shown in Tables 2.4-5.

Table 2.4. Characteristics of different Silver nanoparticles (AgNPs) made from Formaldehyde as a function of 3-APTMS concentration.

S. no.	$AgNO_3$ (M)	3-APTMS (M)	Formaldehyde (M)	AgNPs formation	Extent of formation
A	0.01	$0.1x10^{-3}$	0.8	White	-
B	0.01	0.001	0.8	White	-
C	0.01	0.005	0.8	White	-
D	0.01	0.01	0.8	White	-
E	0.01	0.05	0.8	Grey	-
F	0.01	0.1	0.8	Dark Grey	-
G	0.01	0.25	0.8	Light Yellow	+++
H	0.01	0.5	0.8	Yellow ($AgNP_6$)	+++
I	0.01	1	0.8	Yellow	++++
J	0.01	2	0.8	Dark Yellow	++++

Table 2.5. Characteristics of different Silver nanoparticles (AgNPs) as a function of Formaldehyde concentration.

S. No.	$AgNO_3$ (M)	3-APTMS (M)	Formaldehyde (M)	AgNPs formation	Extent of formation
a	0.01	2	0.4	Dark Yellow	++
b	0.01	2	0.8	Dark Yellow	+++++
c	0.01	2	1.2	Dark Yellow	+++

2.2.3 Measurements and Characterizations

The absorption spectra of samples were recorded in corresponding solvents using a Hitachi U-2900 Spectrophotometer. Transmission electron microscopy (TEM) studies were performed using Hitachi 800 and 8100 electron microscopes (Tokyo, Japan) with an acceleration voltage of 200 kV and Philips CM 200 Supertwin TEM. For the TEM measurement, a few drops of AgNPs were put over a carbon coated copper grid. Measurements were performed on these grids after drying the samples naturally. The Fourier transform infrared (FTIR) spectra of sample was performed on

Perkin Elmer spectrum 100 IR spectrometer using the KBr pellet method in the range of 500 cm^{-1} to 4000 cm^{-1}. Energy dispersive X-ray spectroscopy (EDX) analysis was conducted with FEI Quanta 200 F to perform the quantitative analysis of material.

2.3. RESULTS

2.3.1. GPTMS and 3-APTMS mediated synthesis of AgNPs

In order to synthesize the AgNPs, the interaction of APTMS and GPTMS is analyzed by UV-Vis spectra. The results based on UV-Vis spectra shows in Figure 2.1. and 2.2 for the interaction between GPTMS and 3-APTMS are as follows; (i) constant concentrations of GPTMS followed by subsequent addition of 3-APTMS; (ii) constant concentrations of 3-APTMS followed by subsequent addition of GPTMS. Such interaction of GPTMS to 3-APTMS is confirmed due to appearance of prominent new peak at~280 nm which is evaluated from the reaction product as shown in Figure 2.2 while very weak interaction as evidenced from absorption at 280 nm [Figure 2.1.], was observed when there is addition of 3-APTMS to GPTMS. Subsequent investigation is to understand the role of $AgNO_3$ on the interaction dynamics of 3-APTMS and GPTMS, if any. For this, the reaction system as shown in Figure 2.1 and 2.2 is again recorded in the presence of 0.025 M $AgNO_3$ and the finding is recorded in Figures 2.3 and 2.4. Further, Figure 2.5 shows the visual photographs of AgNPs made by constant concentration of $AgNO_3$ (25 mM) and different compositions of 3-APTMS/GPTMS (Table 2.1).

In order to compare the synthesis of AgNPs with AuNPs synthesis [Pandey *et al*., (2014a)], the following UV-Vis studies has also been done. Figure 2.6. and 2.7 shows the result on step 1-interaction of noble metal ions with 3-APTMS, subsequently Figures 2.8 and 2.9 shows the result on step 2- interaction of 3-APTMS capped noble metal ions with GPTMS and final result are found as; (a) there is an appearance of new peak at 380 nm during the interaction of gold ions and 3-APTMS (Figure 2.6.curve-ii) which is absent under similar case with Ag^{+} ions (Figure 2.7. curve-ii), (b) based on the appearance of new peak at 280 nm (Figure 2.9. curves-i, ii, iii), 3-APTMS capped silver ions get converted into AgNPs at relatively faster rate

with GPTMS as compared to that of the same with gold ions (Figure 2.8. curves-i, ii, iii), under similar conditions.

2.3.1.1. Characterization

Figure 2.10 (a) and (b) shows the TEM and particle size distribution for AgNPs made by 0.05 M 3-APTMS and 4 M of GPTMS. Figure 2.11(a) and (b) shows the TEM and particle size distribution for AgNPs made by 0.5 M 3-APTMS and 4 M of GPTMS. Figure 2.12(a) and (b) shows the TEM and particle size distribution for AgNPs made by 0.5 M 3-APTMS and 2 M of GPTMS. The finding shows the average size of AgNPs close to 4.7 nm at 0.05 M 3-APTMS (Figure 2.10) whereas 7.7 nm when 3-APTMS is increased to 0.5 M (Figure 2.11) and confirm the dependence of nanogeometry on 3-APTMS concentrations while 8.9 nm when 3-APTMS is increased to 0.5 M and 2 M of GPTMS (Figure 2.12). Figure 2.13 shows the EDX of AgNPs and justify the presence of Ag with silica content.

2.3.1.2. Dispersibility of AgNPs in Aqueous and Non-Aqueous Medium

The next phase of investigations is to understand the dispersibility of as synthesized AgNPs of two different sizes in the solvents of variable refractive index. Figure 2.14 shows the UV-Vis spectra of AgNPs of two different sizes; $AgNP_1$ of 4.7 nm and $AgNP_3$ of 8.9 nm in methanol and butanol. Figure 2.15 shows the UV-Vis spectra of AgNPs of the same in acetonitrile and dichloromethane. Two common solvents were chosen for understand the dispersibility of as synthesized AgNPs, having polarity at extreme ends i.e., Water and Toluene. As synthesized AgNPs based on the composition of 3-APTMS and GPTMS (Table 2.1) may be categorized into three parts; (i) better dispersibility of AgNPs in water as compared to that of toluene (ii) better dispersibility of AgNPs in toluene as compared to that of water and (iii) relatively better dispersibility in toluene and non dispersible in water. The UV-Vis spectra and visual images of AgNPs based such trends are shown in Figures 2.16-21 and the extent of dispersibility of the same in respective solvents are recorded in Tables 2.6–8 respectively.

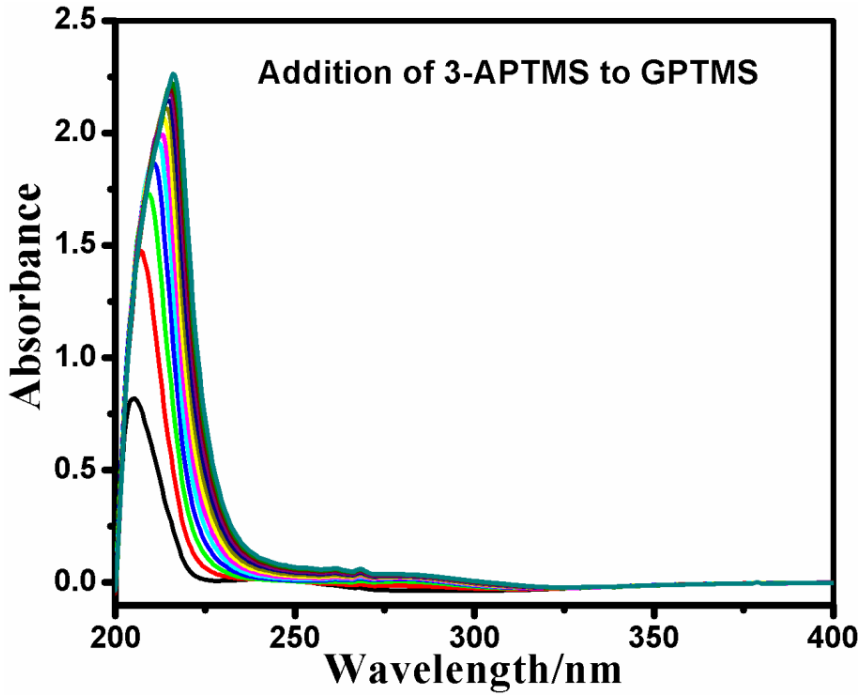

Figure 2.1. UV-Vis absorption spectra for the interaction between increasing concentrations of 3-APTMS into constant methanolic suspension of GPTMS.

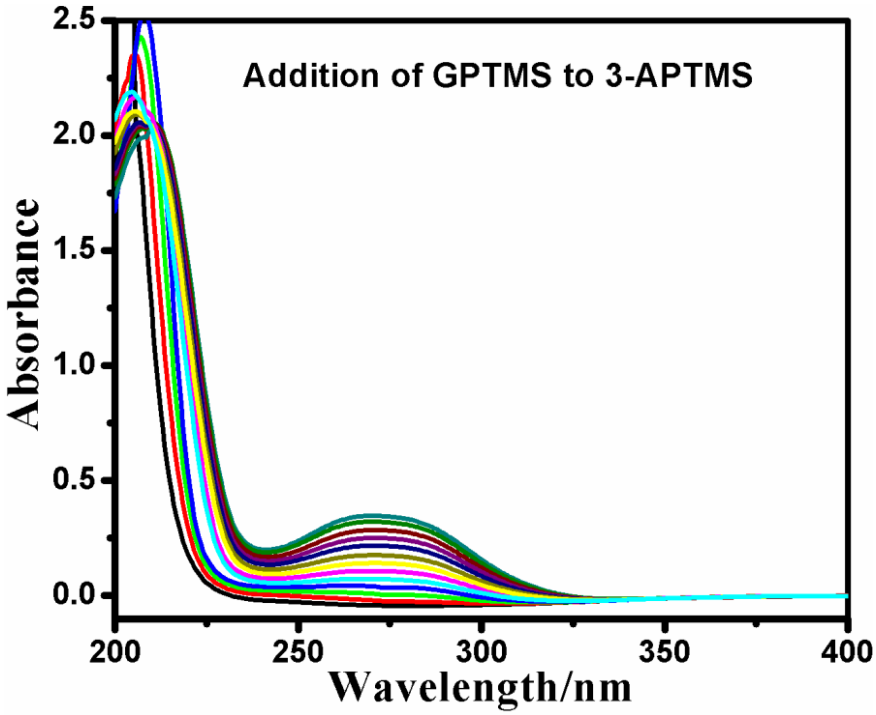

Figure 2.2. UV-Vis absorption spectra for the interaction between increasing concentrations of GPTMS into constant methanolic suspension of 3-APTMS.

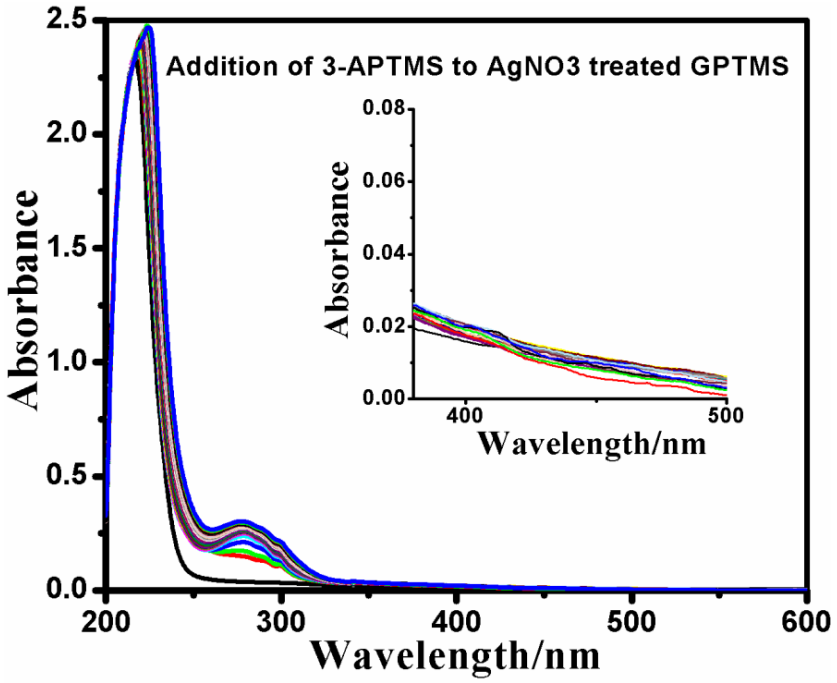

Figure 2.3. UV-Vis absorption spectra for the interaction between increasing concentrations of 3-APTMS into constant methanolic suspension of GPTMS containing Ag^{+}. Inset shows the respective recording between 380–500 nm.

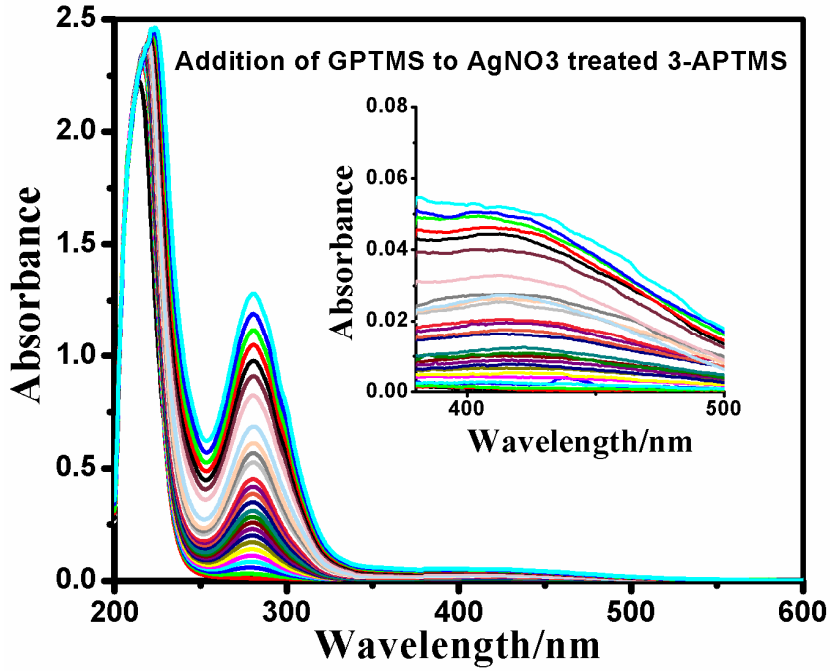

Figure 2.4. UV-Vis absorption spectra for the interaction between increasing concentrations of GPTMS into constant methanolic suspension of 3-APTMS containing Ag^{+}. Inset shows the respective recording between 380–500 nm.

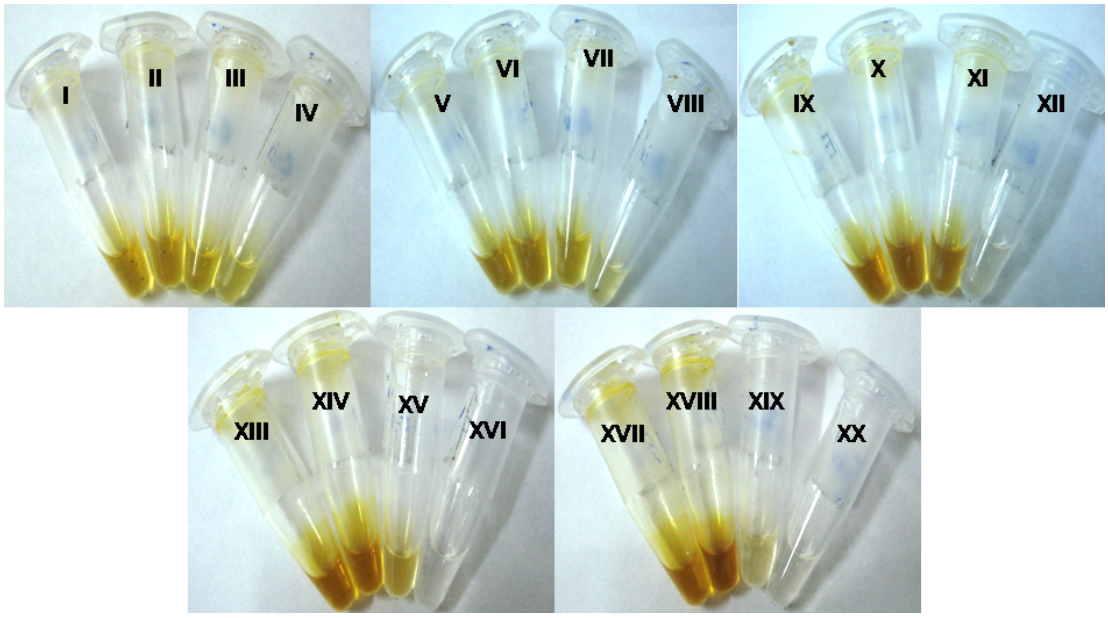

Figure 2.5. Visual photographs of AgNPs made by using composition of 3-APTMS, GPTMS and $AgNO_3$ as shown in Table 2.1 for respective samples.

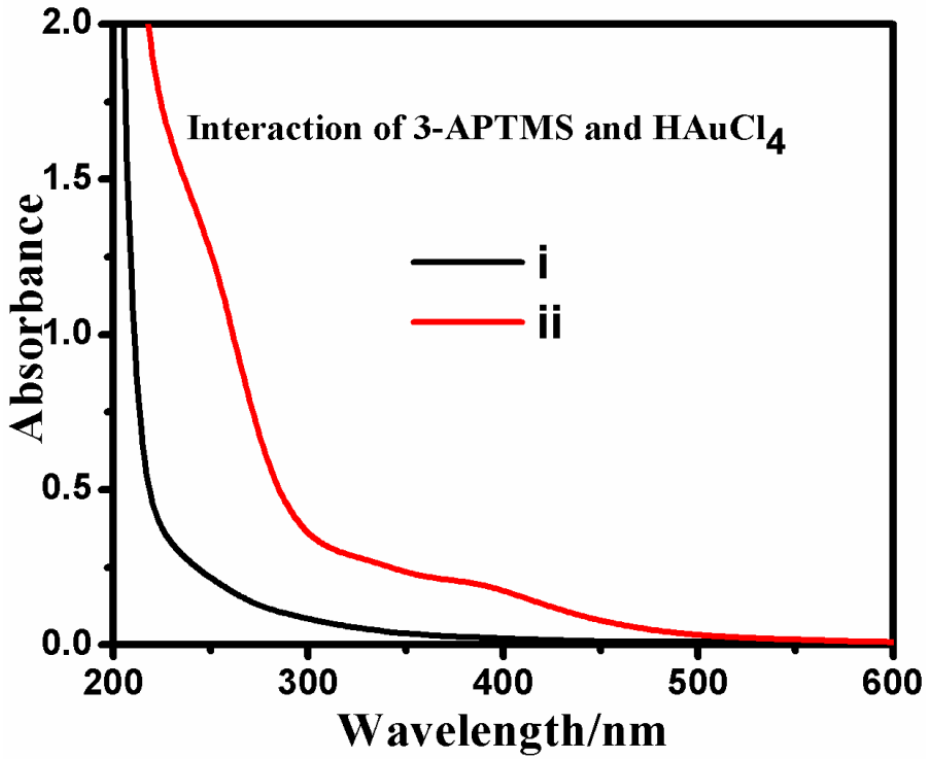

Figure 2.6. Variation in absorbance as function of wavelength on the subsequent additions of 3-APTMS (i) and 0.025 M $HAuCl_4$ (ii).

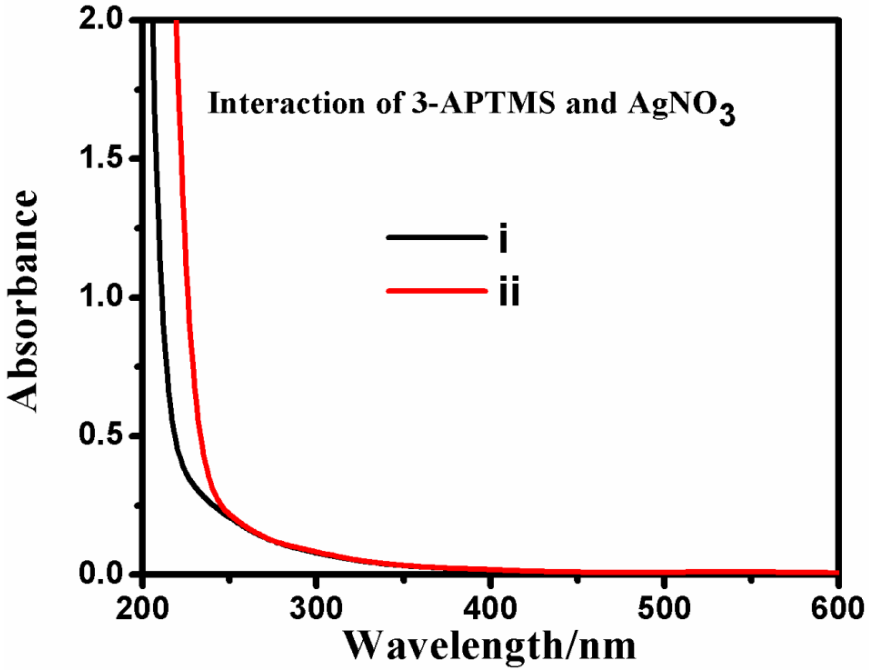

Figure 2.7. Variation in absorbance as function of wavelength on the subsequent additions of 3-APTMS (i) and 0.025 M $AgNO_3$ (ii).

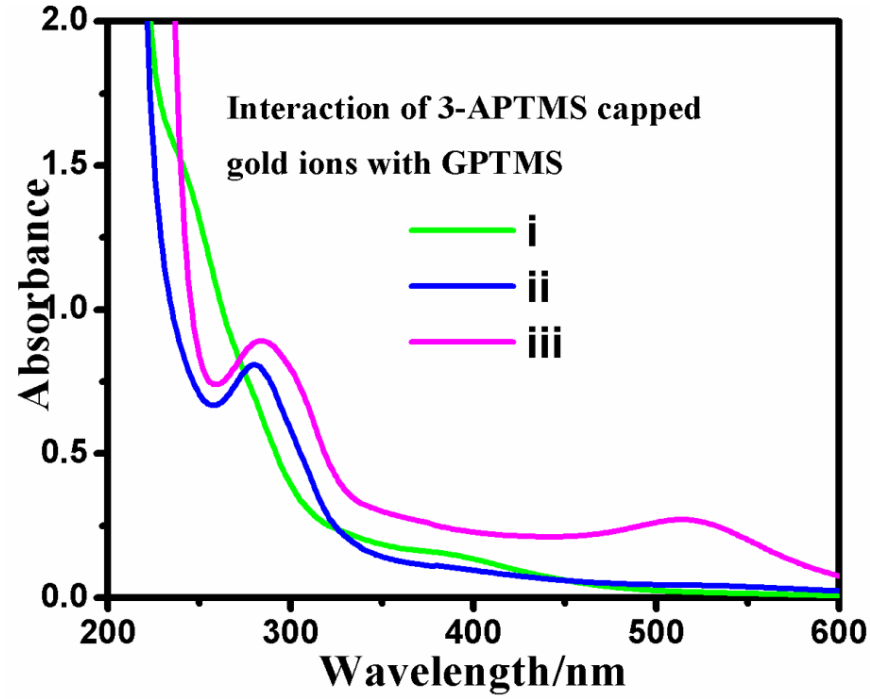

Figure 2.8. The change in absorbance after immediate addition of GPTMS in 3-APTMS capped gold ions (i) followed by subsequent recording of change in absorbance as a function of time:after 1 h (ii) and 6 h (iii).

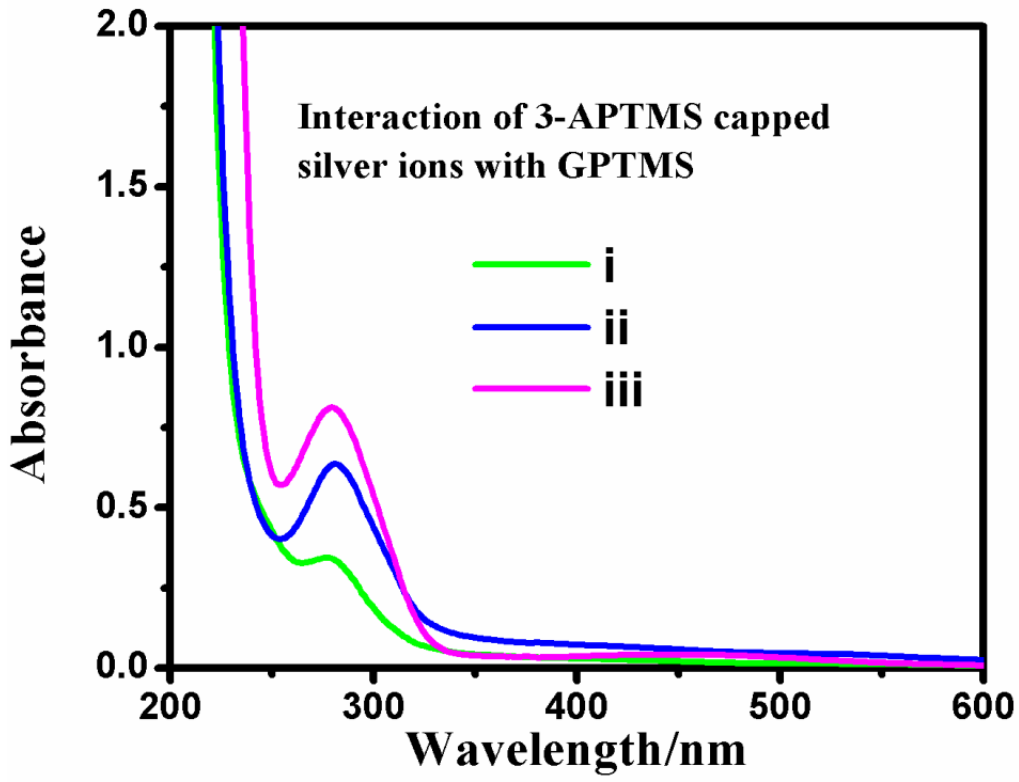

Figure 2.9. The change in absorbance after immediate addition of GPTMS in 3-APTMS capped silver ions (i) followed by subsequent recording of change in absorbance as a function of time: after 1 h (ii) and 6h (iii).

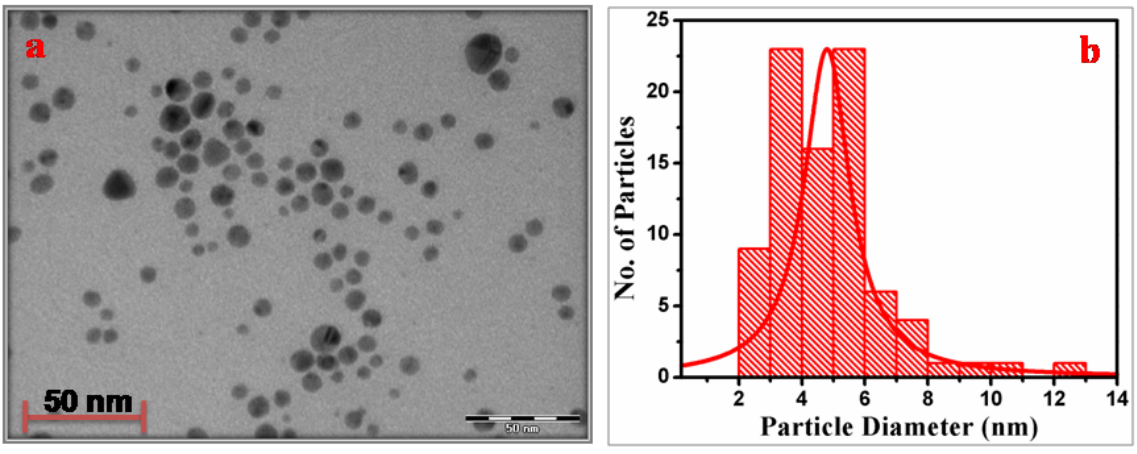

Figure 2.10. (a) TEM image of AgNPs made by 0.05 M 3-APTMS and 4 M GPTMS; (b) particle size distribution.

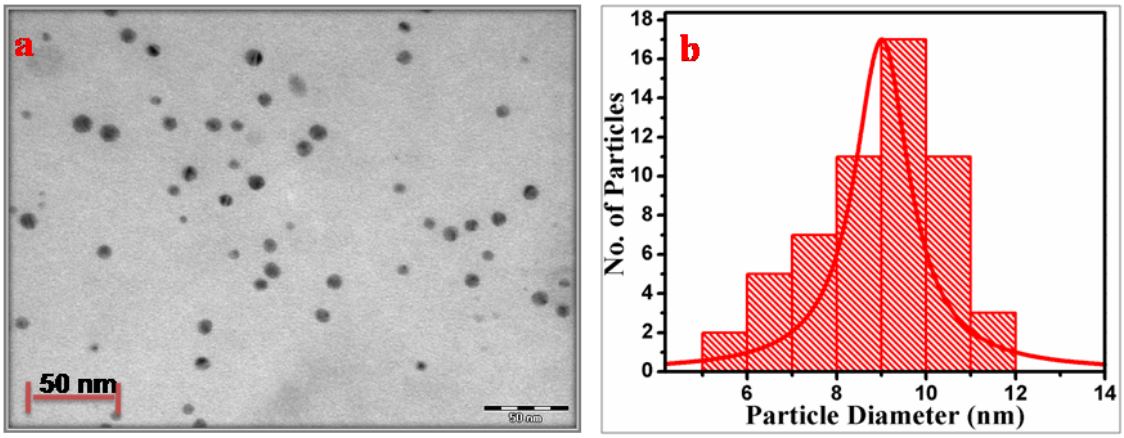

Figure 2.11. (a) TEM image of AgNPs made by 0.5 M 3-APTMS and 4 M GPTMS; (b) particle size distribution.

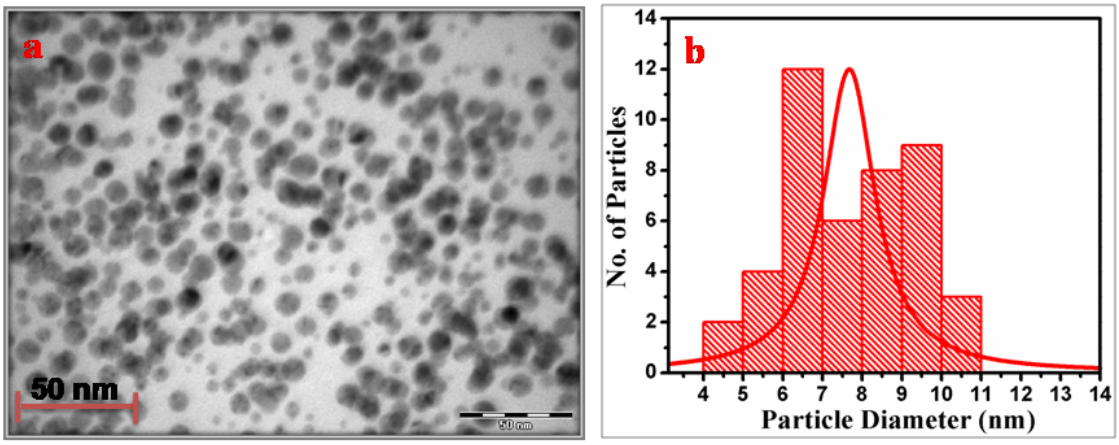

Figure 2.12. (a) TEM image of AgNPs made by 0.5 M 3-APTMS and 2 M GPTMS; (b) particle size distribution.

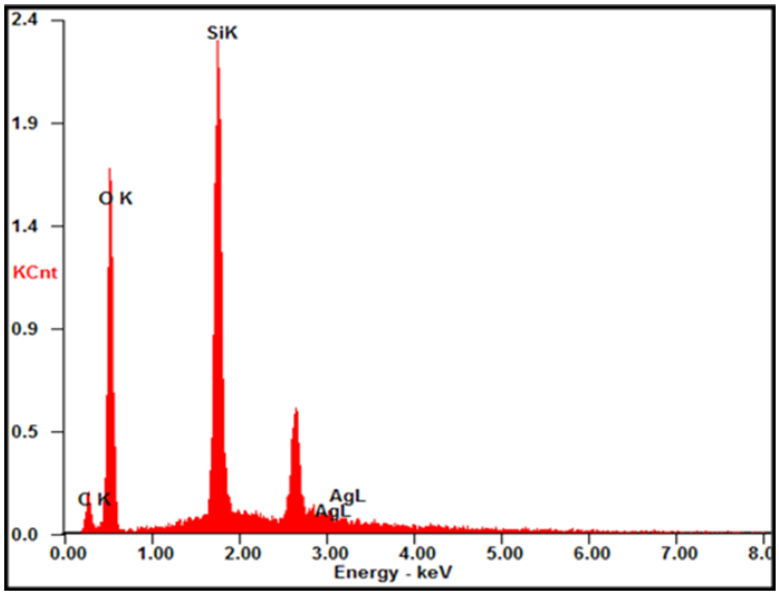

Figure 2.13. Image shows the EDX of AgNPs.

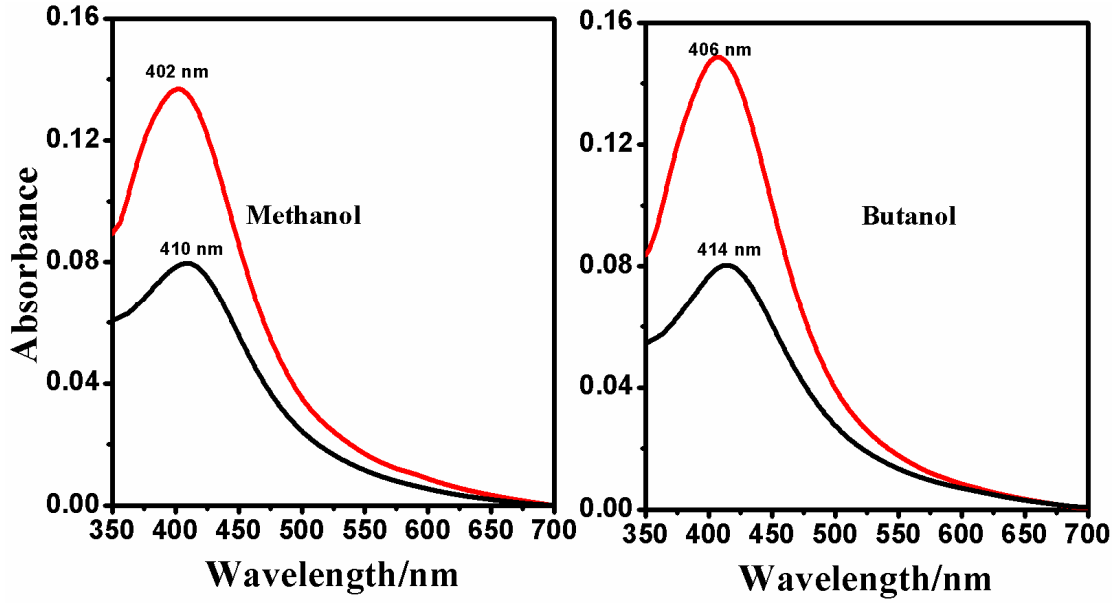

Figure 2.14. UV-Vis absorption spectra of $AgNP_1$ and $AgNP_3$ in methanol and butanol. The curve as shown with red line represents the variation in absorbance in different solvents for $AgNP_1$ (λ_{max} 402 and 406 nm) and the curves with black line represent for $AgNP_3$ (λ_{max} 410 and 414 nm).

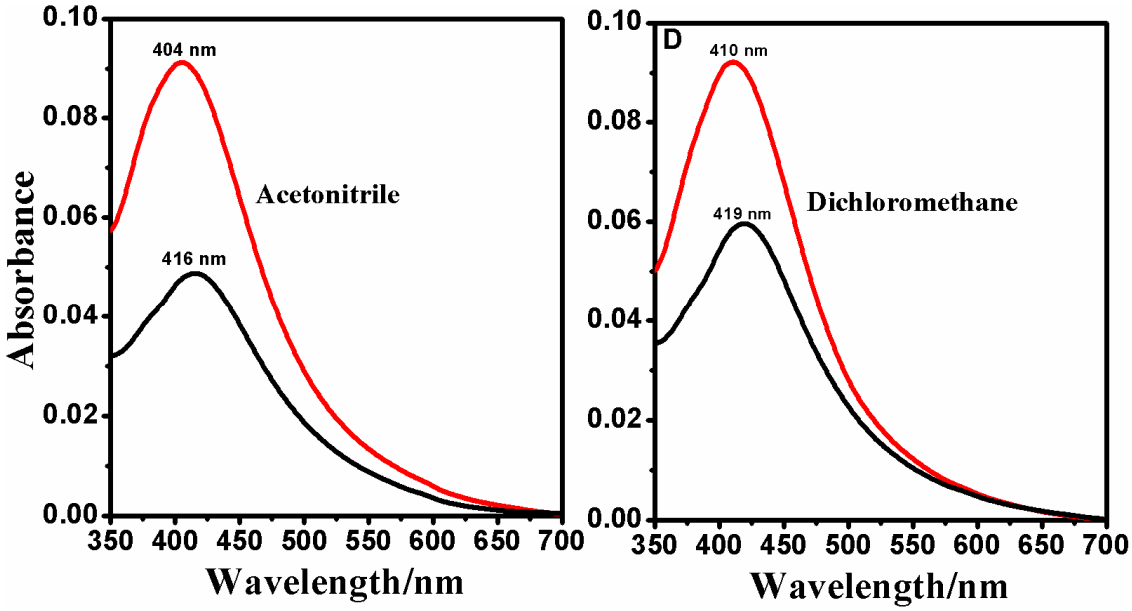

Figure 2.15. UV-Vis absorption spectra of $AgNP_1$ and $AgNP_3$ in acetonitrile and dichloromethane. The curve as shown with red line represents the variation in absorbance in different solvents for $AgNP_1$ (λ_{max} 404 and 410 nm) and the curves with black line represent for $AgNP_3$ (λ_{max} 416 and 419 nm).

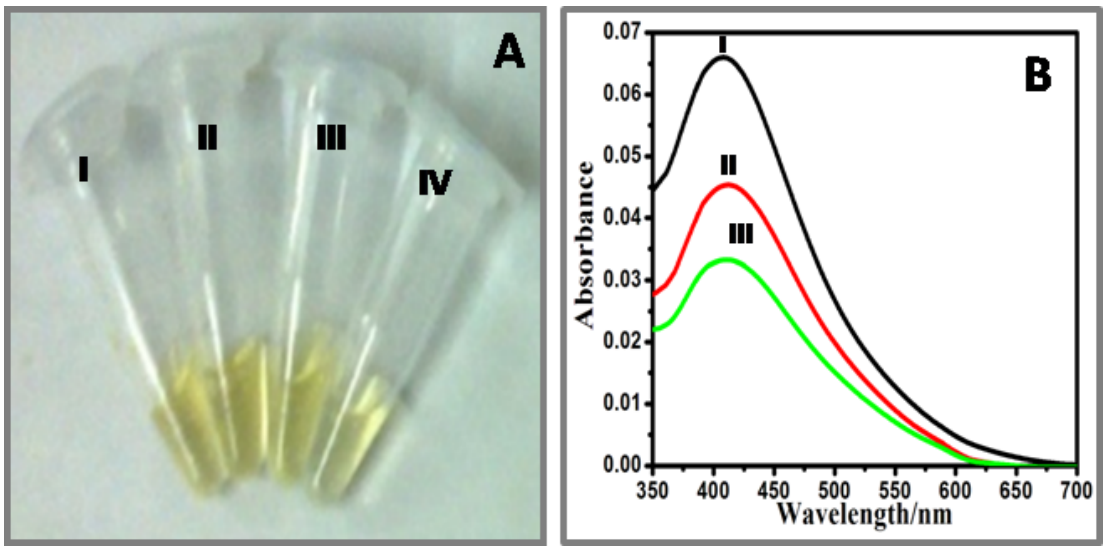

Figure 2.16. (A) Visual photographs of AgNPs made by using composition of 3-APTMS, GPTMS and $AgNO_3$ as shown in Table 2.1. (Sample I–IV) and their dispersibility in water. (B) Shows the UV-Vis spectra of the corresponding sols in water.

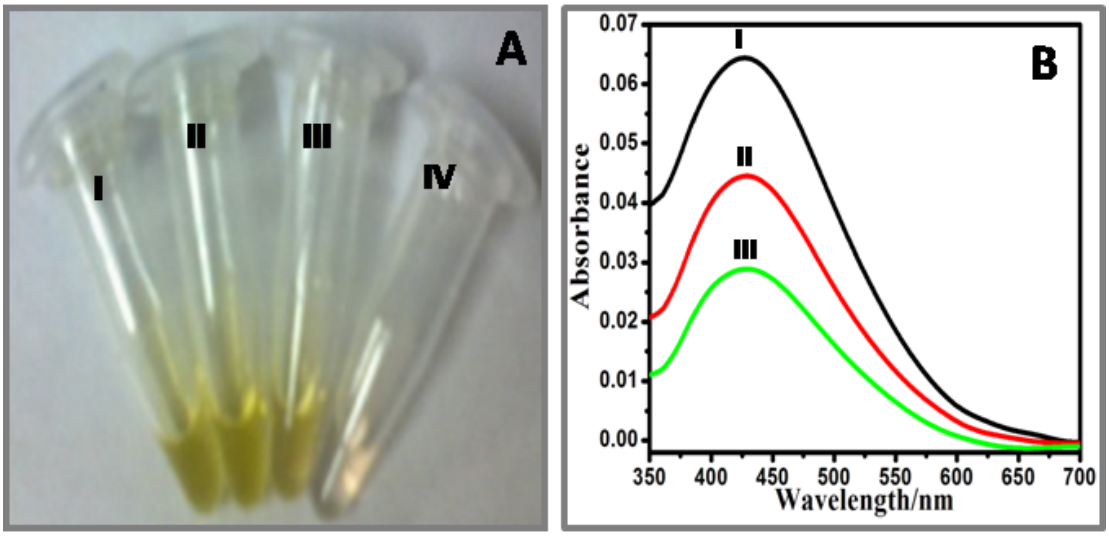

Figure 2.17. (A) Visual photographs of AgNPs made by using composition of 3-APTMS, GPTMS and $AgNO_3$ as shown in Table 2.1. (Sample I–IV) and their dispersibility in toluene. (B) Shows the UV-Vis spectra of the corresponding sols in toluene.

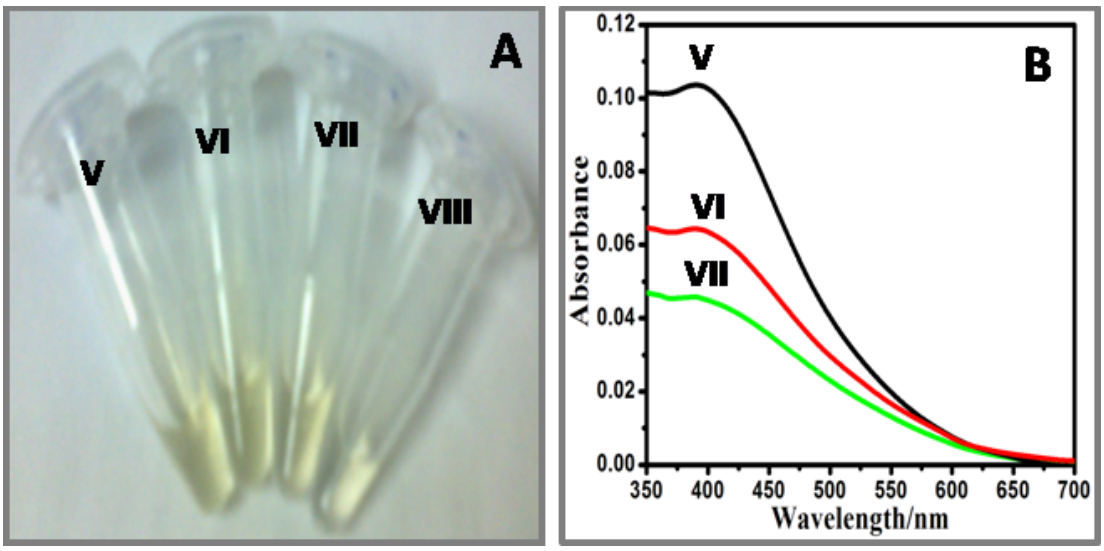

Figure 2.18. (A) Visual photographs of AgNPs made by using composition of 3-APTMS, GPTMS and $AgNO_3$ as shown in Table 2.1. (Sample V-VIII) and their dispersibility in water. (B) Shows the UV-Vis spectra of the corresponding sols in water.

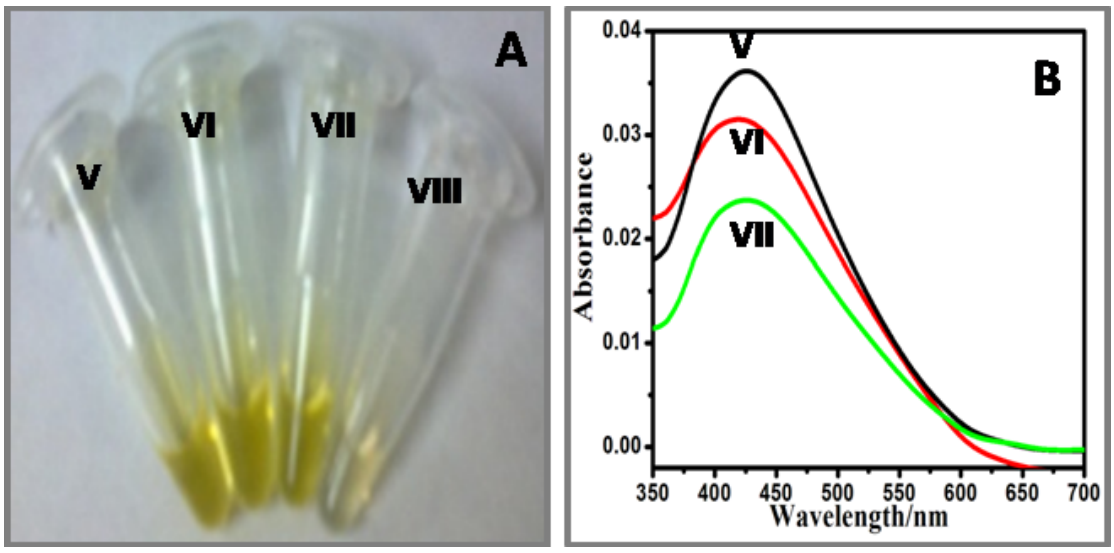

Figure 2.19. (A) Visual photographs of AgNPs made by using composition of 3-APTMS, GPTMS and $AgNO_3$ as shown in Table 2.1. (Sample V-VIII) and their dispersibility in toluene. (B) Shows the UV-Vis spectra of the corresponding sols in toluene.

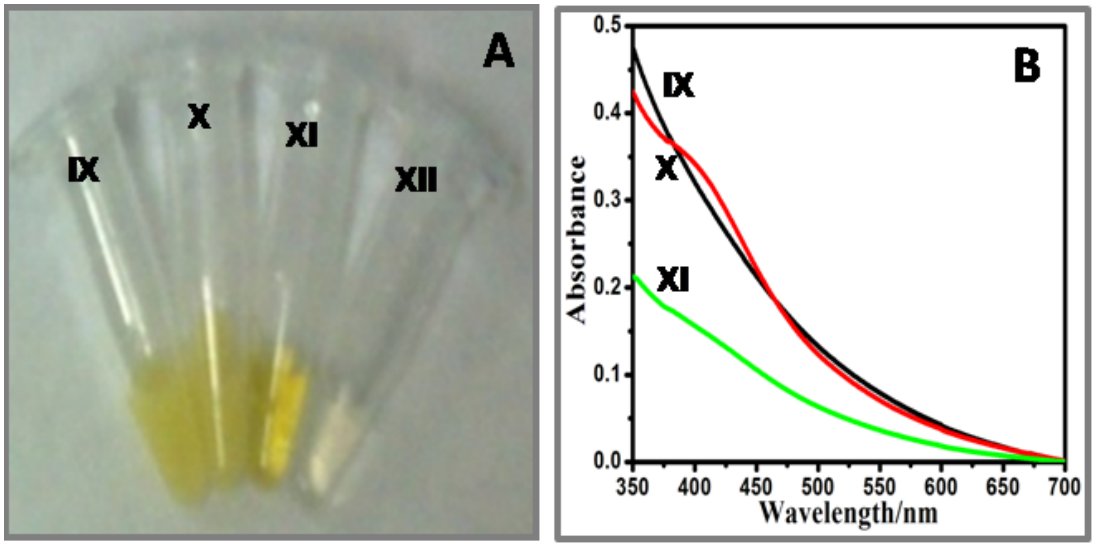

Figure 2.20. Visual photographs of AgNPs made by using composition of 3-APTMS, GPTMS and $AgNO_3$ as shown in Table 2.1. (Sample IX–XII) and their dispersibility in water. (B) Shows the UV-Vis spectra of the corresponding sols in water.

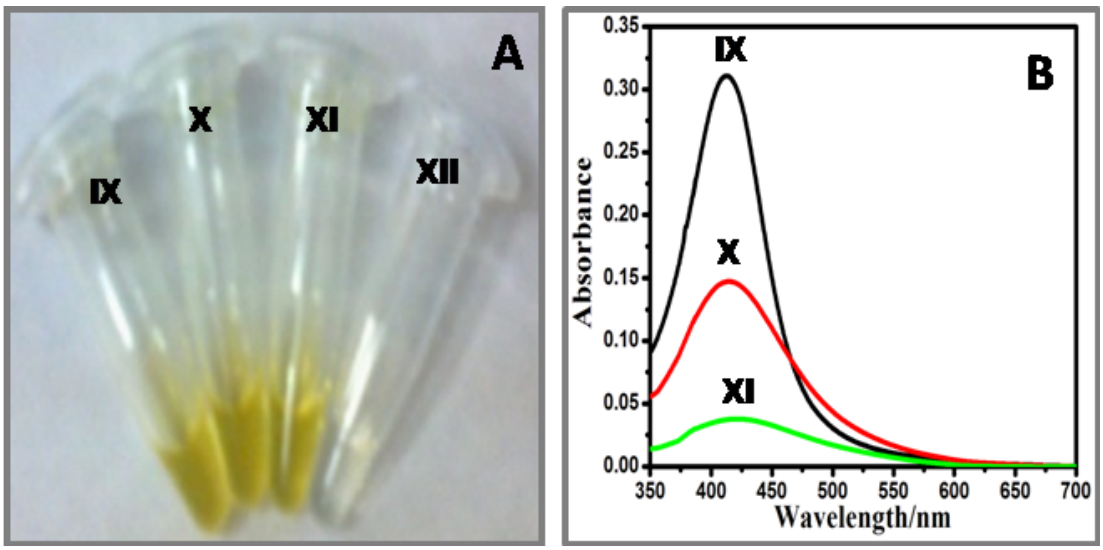

Figure 2.21. Visual photographs of AgNPs made by using composition of 3-APTMS, GPTMS and $AgNO_3$ as shown in Table 2.1. (Sample IX–XII) and their dispersibility in toluene. (B) Shows the UV-Vis spectra of the corresponding sols in toluene.

Table 2.6. Dispersibility of AgNPs in toluene and water made by using constant concentrations of 3-APTMS (0.05 M) and varying concentrations of GPTMS. "+" and "-" sign denotes increasing and decreasing extent of AgNPs dispersibility in water and toluene.

Sample Name	3-APTMS mol dm^{-3}	GPTMS mol dm^{-3}	Dispersibility	
			Toluene	Water
I	0.05	4	+	++
II	0.05	3	+	++
III	0.05	2	+	++
IV	0.05	1	+	++

Table 2.7. Dispersibility of AgNPs in toluene and water made by using constant concentrations of 3-APTMS (0.1 M) and varying concentrations of GPTMS. "+" and "-" sign denotes increasing and decreasing extent of AgNPsdispersibility in water and toluene.

Sample Name	3-APTMS mol dm^{-3}	GPTMS mol dm^{-3}	Dispersibility	
			Toluene	Water
V	0.1	4	++	+
VI	0.1	3	++	-
VII	0.1	2	++	-
VIII	0.1	1	++	-

Table 2.8. Dispersibility of AgNPs in toluene and water made by using constant concentrations of 3-APTMS (0.5 M) and varying concentrations of GPTMS. "+" and "-" sign denotes increasing and decreasing extent of AgNPsdispersibility in water and toluene.

Sample Name	3-APTMS mol dm^{-3}	GPTMS mol dm^{-3}	Dispersibility	
			Toluene	Water
IX	0.5	4	+++	---
X	0.5	3	++	---
XI	0.5	2	+	---
XII	0.5	1	+	---

2.3.2. 3-APTMS and Cyclohexanone/Formaldehyde mediated synthesis of AgNPs

In the previous sections (2.3.1), we have demonstrated that the controlled synthesis of AgNPs can be obtained by involving the active role 3-APTMS and GPTMS. There is use of both alkoxysilane which increases the silane content and limits the AgNPs for various practical applications. Accordingly, we intended to understand the role of other organic moieties that allow the conversion of silver ion into AgNPs. Fortunately, we found that Cyclohexanone and formaldehyde provide controlled conversion of silver nitrate into AgNPs in presence of 3-APTMS. The role of cyclohexanone / formaldehyde on real time conversion of 3-APTMS capped silver ions has been studied. The formation of AgNPs in the presence of 3-APTMS and cyclohexanone under two different conditions; (1) keeping constant concentration of cyclohexanone while changing the concentration of 3-APTMS and (2) keeping 3-APTMS constant while changing the concentrations of cyclohexanone are studied as shown in previous section 2.2.2.2 in the form of tables while their corresponding photographs in Figure 2.22 and Figure 2.23. Subsequently, Figure 2.24 and Figure 2.25 shows the real time synthesis of AgNPs mediated by 3- APTMS and formaldehyde at lower concentration of 3-APTMS (0.5 M), whereas Figure 2.25

shows the similar result at 2M APTMS. Further, the synthesis of AgNPs in the presence of 3-APTMS and formaldehyde under two different conditions; (1) keeping constant concentration of formaldehyde while changing the concentration of 3-APTMS; and (2) keeping 3-APTMS constant while changing the concentrations of formaldehyde; are studied as shown in previous section 2.2.2.3 in the form of tables while their corresponding photographs and UV-Vis spectra in Figure 2.26-27.

2.3.2.1. Characterization

The as synthesized $AgNP_4$ were characterized by FTIR. A Figure 2.28 depicts the FTIR spectra of AgNPs. The spectrum show absorption band at around 3800, 2800, 1090-1120, 2820-2940, 1220-1275 cm^{-1}. Both 3-APTMS and organic reducing agents control the nanogeometry of AgNPs. The TEM images of as synthesized AgNPs made from 3-APTMS and cyclohexanone at two different concentrations of 3-APTMS are shown in Figure 2.290-2.30 (a) along with selected area electron diffraction (SAED) pattern and (b) the finding shows the spherical shape with average size of 5 nm ($AgNP_4$) and 7 nm ($AgNP_5$) at 0.25 M and 0.5 M APTMS respectively keeping similar concentration of cyclohexanone (1.9 M). The use of hydrophilic organic reducing agent like formaldehyde results homogeneous distribution of $AgNP_6$ having average particle size to the order of 4 nm as shown in Figure 2.31(a) along with SAED pattern (b).

2.3.2.1. Dispersibility of AgNPs

The results on the dispersibility of AgNPs, made from 3-APTMS and cyclohexanone, as a function of their concentrations in water, methanol, acetonitrile, toluene and dichloromethane has been recorded in Figure 2.32-34 revealing linear relation between λ_{max} vs AgNPs concentrations whereas, Figure 2.35-36 shows the dispersibility of AgNPs synthesized by using formaldehyde in place of cyclohexanone in water, methanol, acetonitrile and butanol.

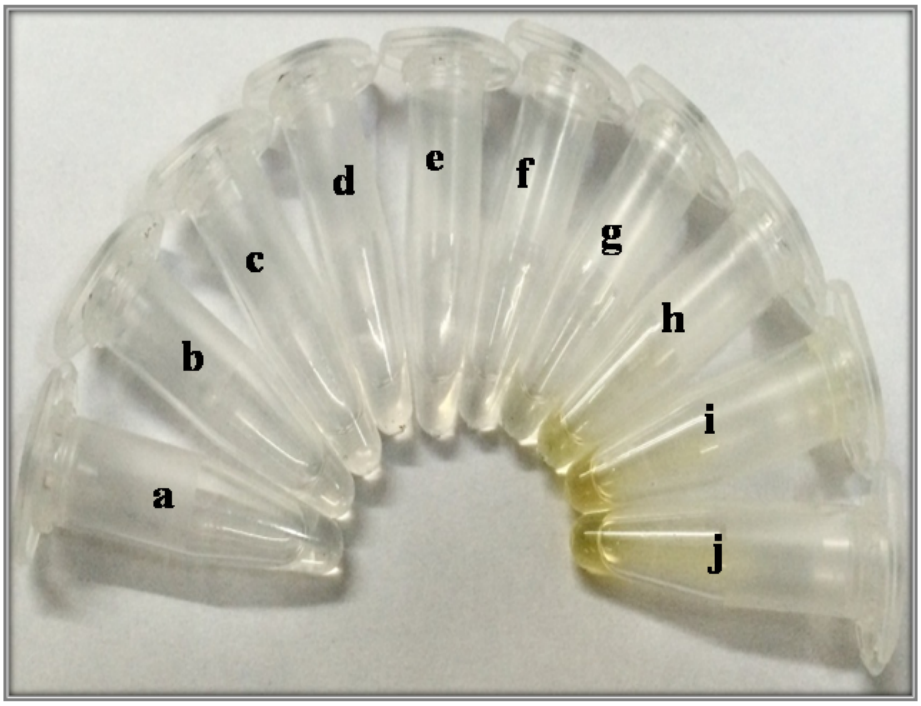

Figure 2.22. The visual photographs of AgNPs containing constant concentrations of $AgNO_3$ (0.01 M) and Cyclohexanone (1.9 M) followed with varying concentrations of 3-APTMS between $0.1x10^{-3}$ M to 2 M (Table 2.2, Sr. no. a to j).

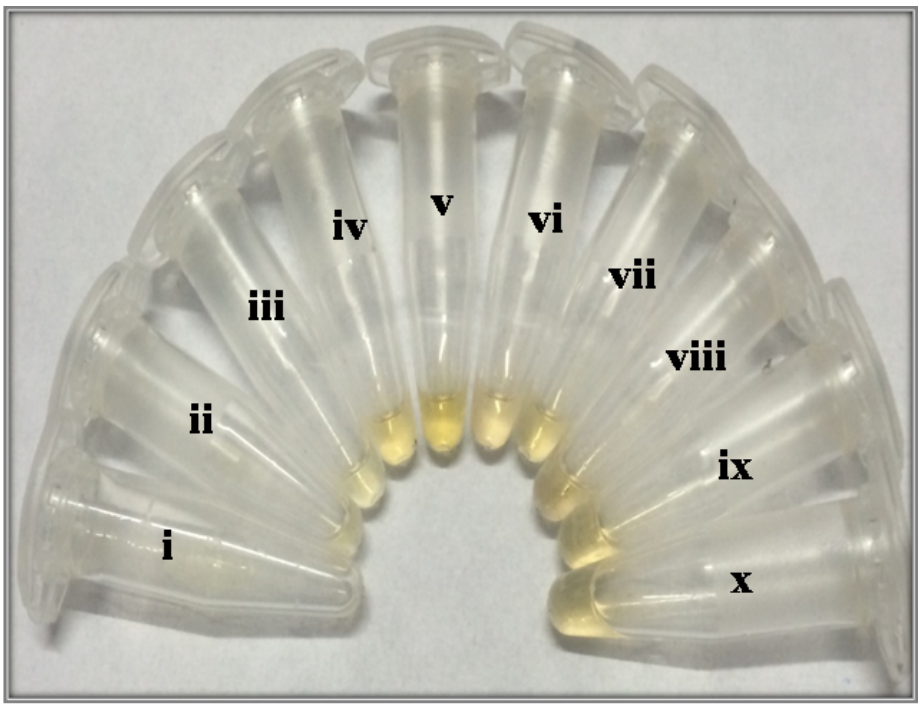

Figure 2.23. The visual photographs of AgNPs containing constant concentrations of $AgNO_3$ (0.01 M) and 3-APTMS (0.5 M) followed with varying concentrations of Cyclohexanone between 0.3 M to 3.8 (Table 2.3, Sr. no. i to x).

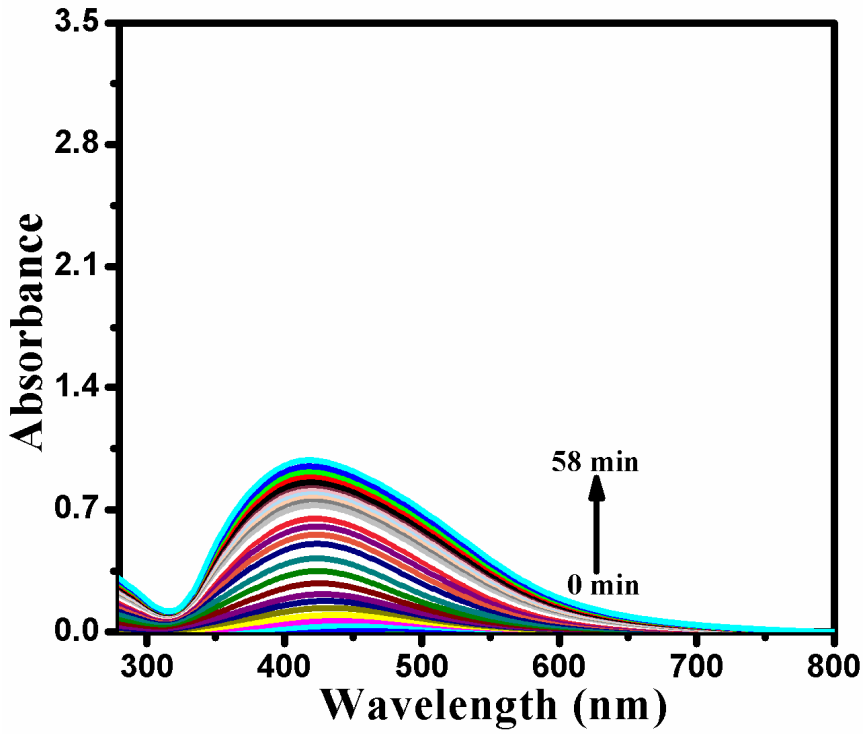

Figure 2.24. Real time synthesis of AgNPs using 0.5 M 3-APTMS and 0.8 M concentration of formaldehyde.

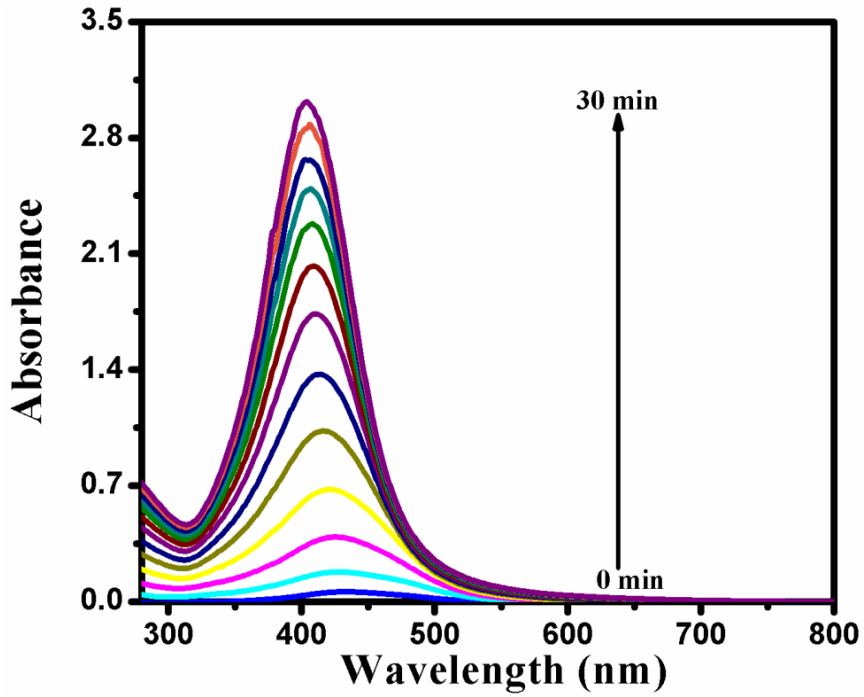

Figure 2.25. Real time synthesis of AgNPs using 2 M 3-APTMS and 0.8 M concentration of formaldehyde.

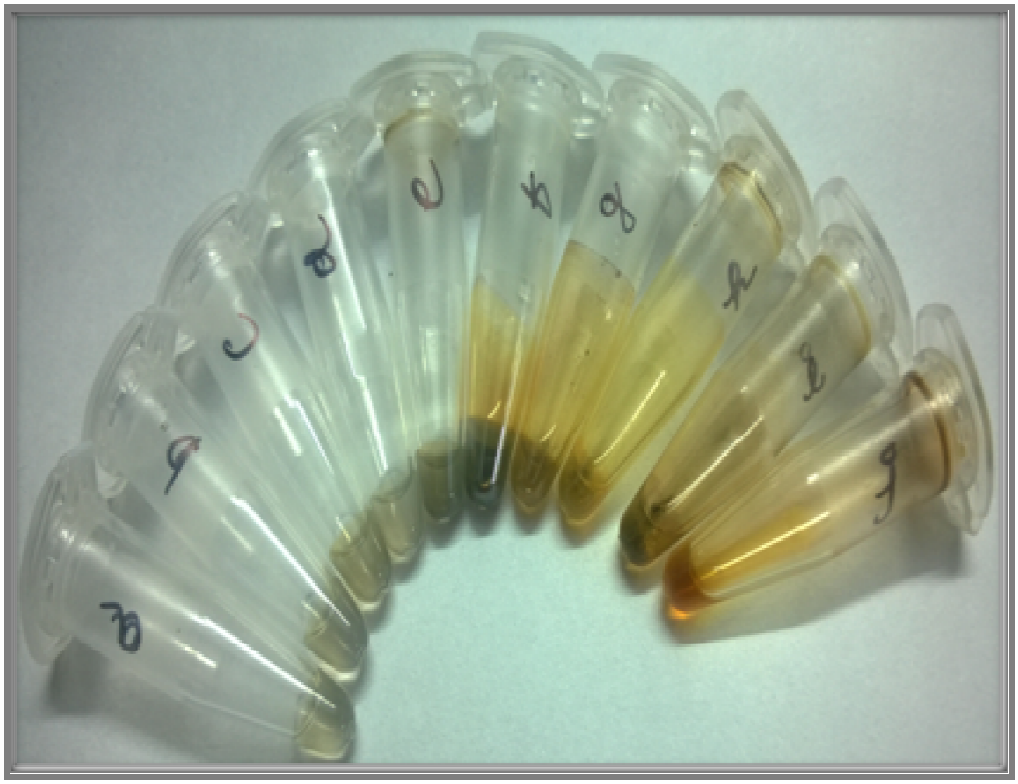

Figure 2.26. Formation of AgNPs as a function of 3-APTMS concentrations (Table 2.4, Sr. no. a to j) keeping constant concentrations of Formaldehyde (0.8 M) and 0.01 M $AgNO_3$.

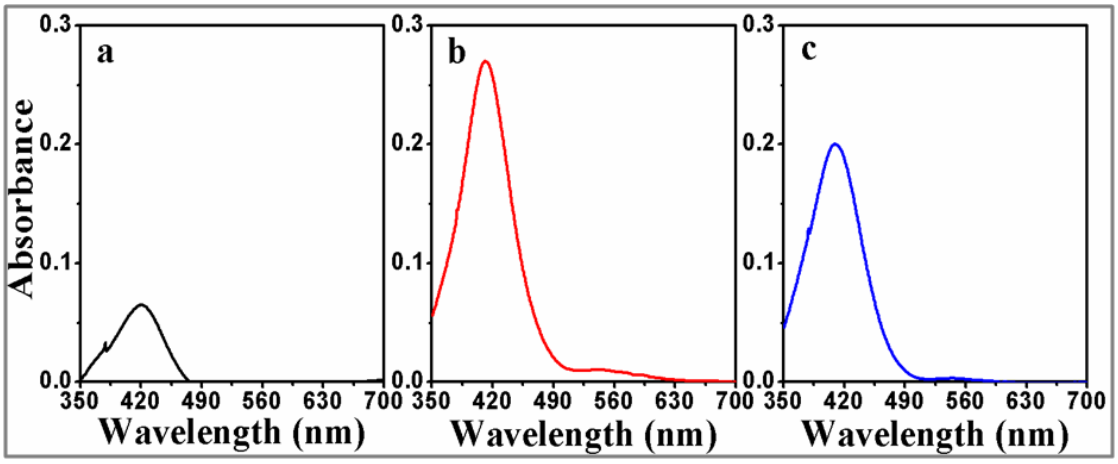

Figure 2.27. Effect of Formaldehyde concentrations on the formation of AgNPs [(a) 0.4 M, (b) 0.8 M and (c) 1.2 M] keeping constant concentration of 3-APTMS (0.5 M).

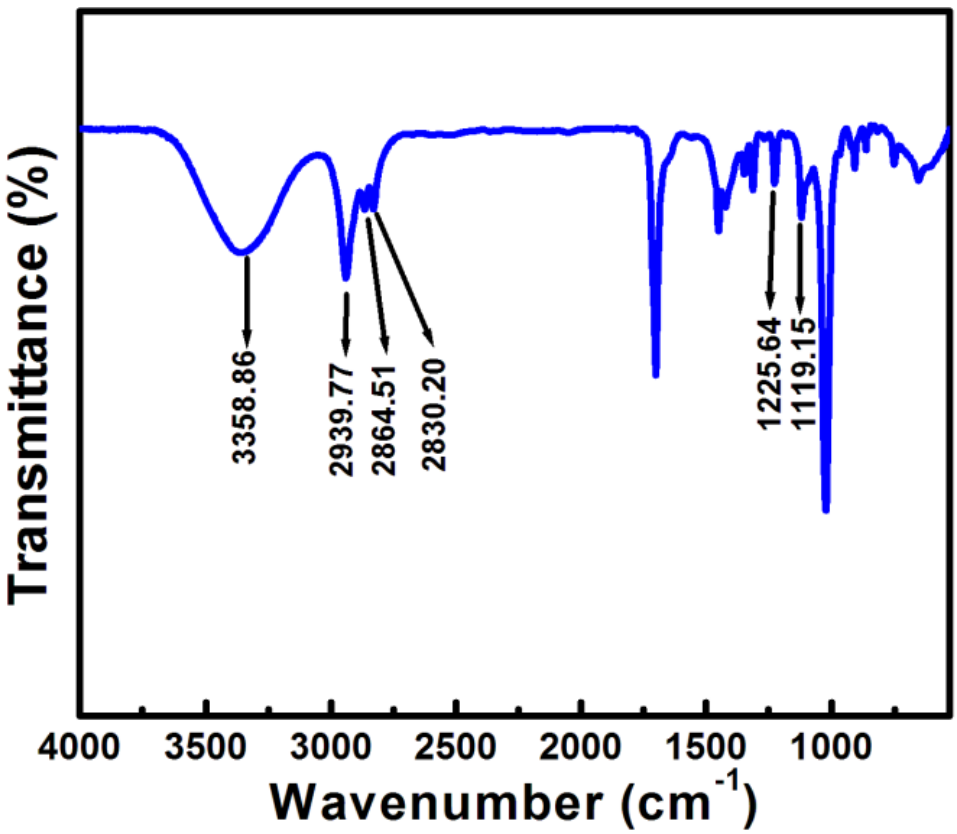

Figure 2.28. FTIR spectrum of AgNPs

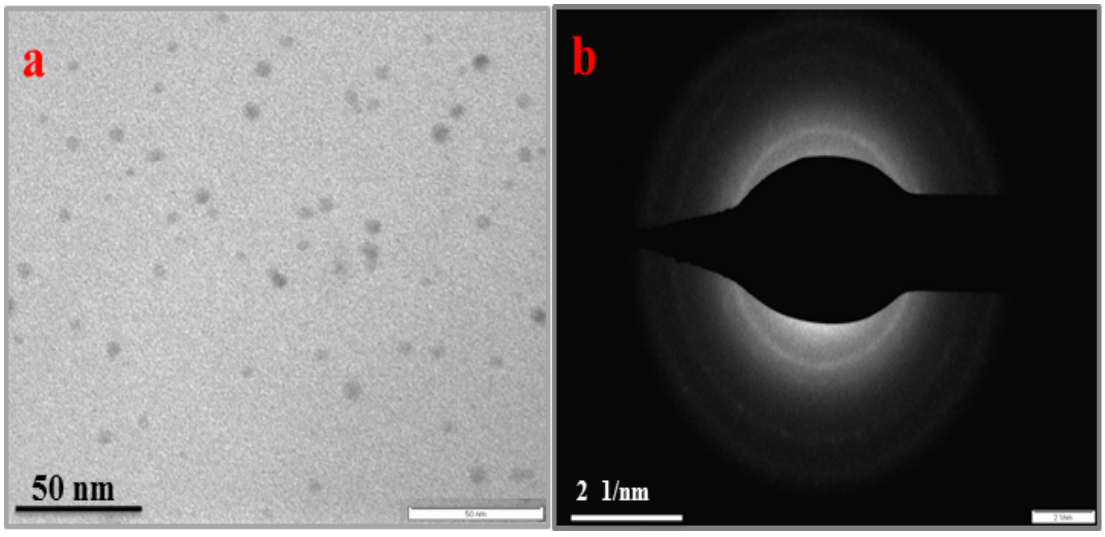

Figure 2.29. TEM (a) and selected area electron diffraction pattern (b) of AgNPs consist of 0.25 M APTMS and fixed concentration of Cyclohexanone.

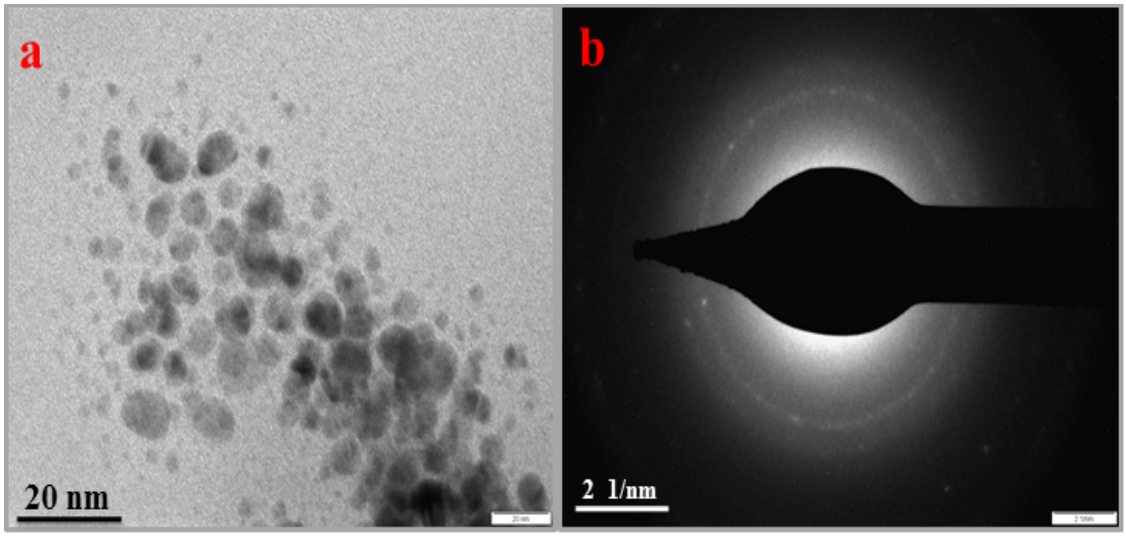

Figure 2.30. TEM (a) and selected area electron diffraction pattern (b) of AgNPs consist of 0.50 M APTMS and fixed concentration of Cyclohexanone.

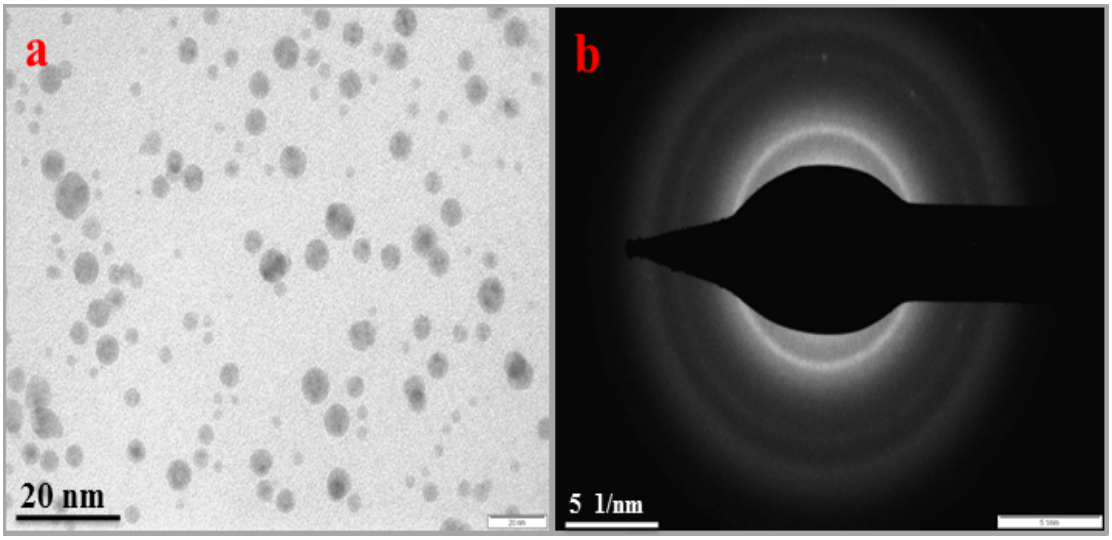

Figure 2.31. TEM (a) and selected area electron diffraction pattern (b) of AgNPs consist of 0.50 M APTMS and fixed concentration of Formaldehyde.

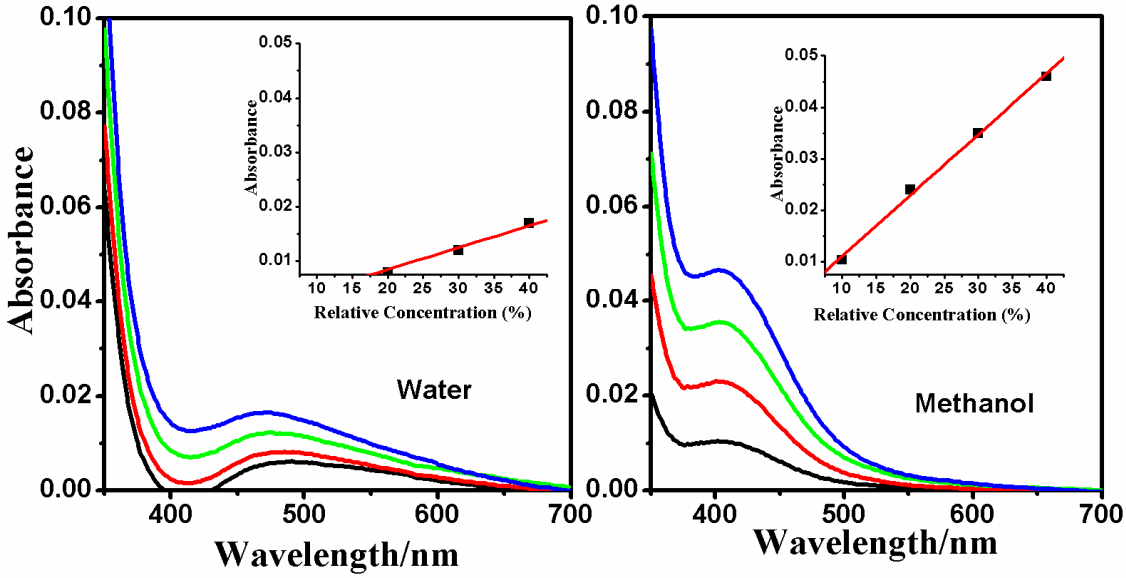

Figure 2.32. UV-Vis absorption spectra of increasing concentrations of AgNPs made from cyclohexanone and 3-APTMS in water and methanol; Respective insets show the dependence of absorption maxima (λ_{max}) on AgNPs concentration.

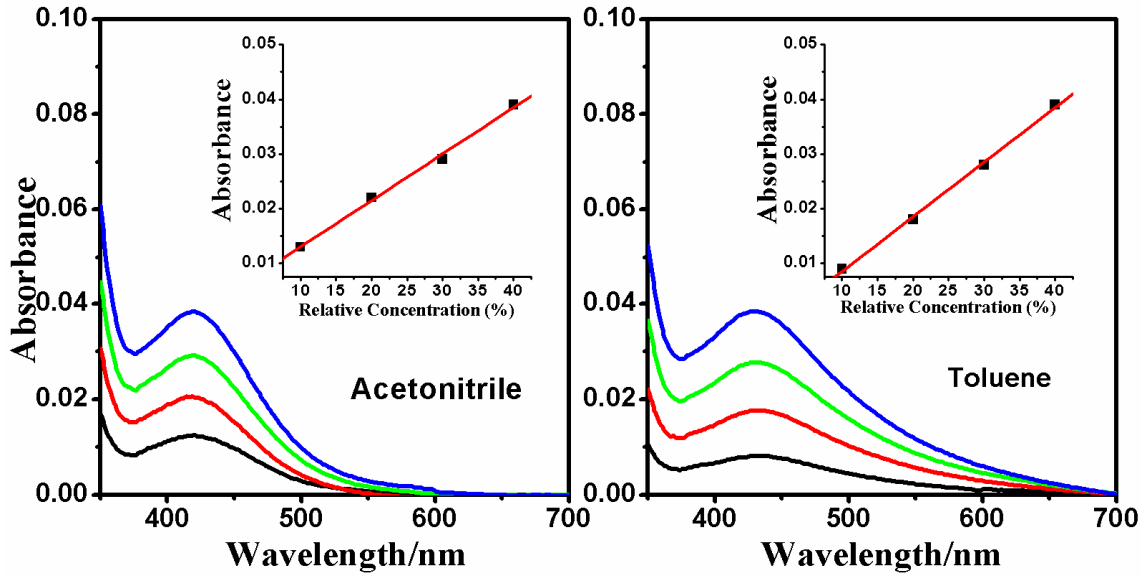

Figure 2.33. UV-Vis absorption spectra of increasing concentrations of AgNPs made from cyclohexanone and 3-APTMS in acetonitrile and toluene; Respective insets show the dependence of absorption maxima (λ_{max}) on AgNPs concentration.

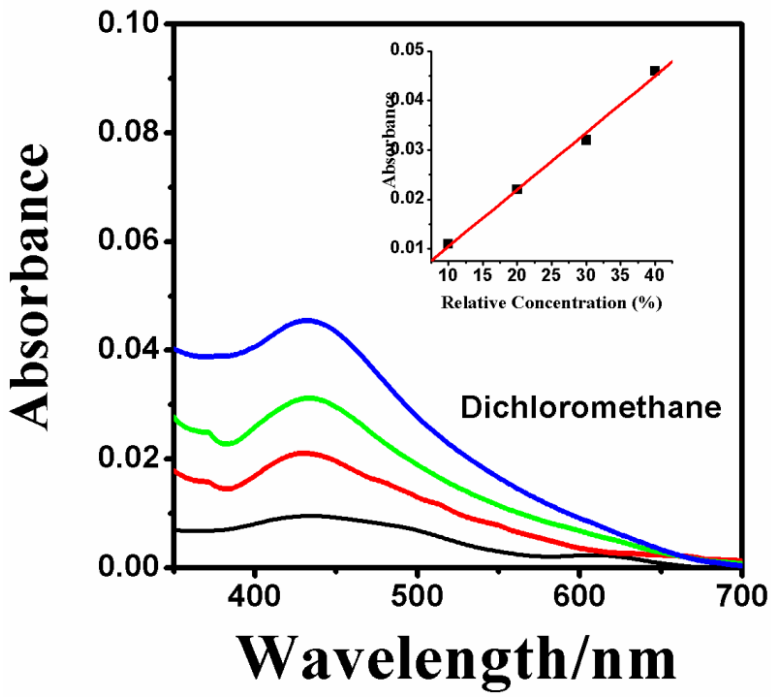

Figure 2.34. UV-Vis absorption spectra of increasing concentrations of AgNPs made from cyclohexanone and 3-APTMS in dichloromethane; Respective inset show the dependence of absorption maxima (λ_{max}) on AgNPs concentration.

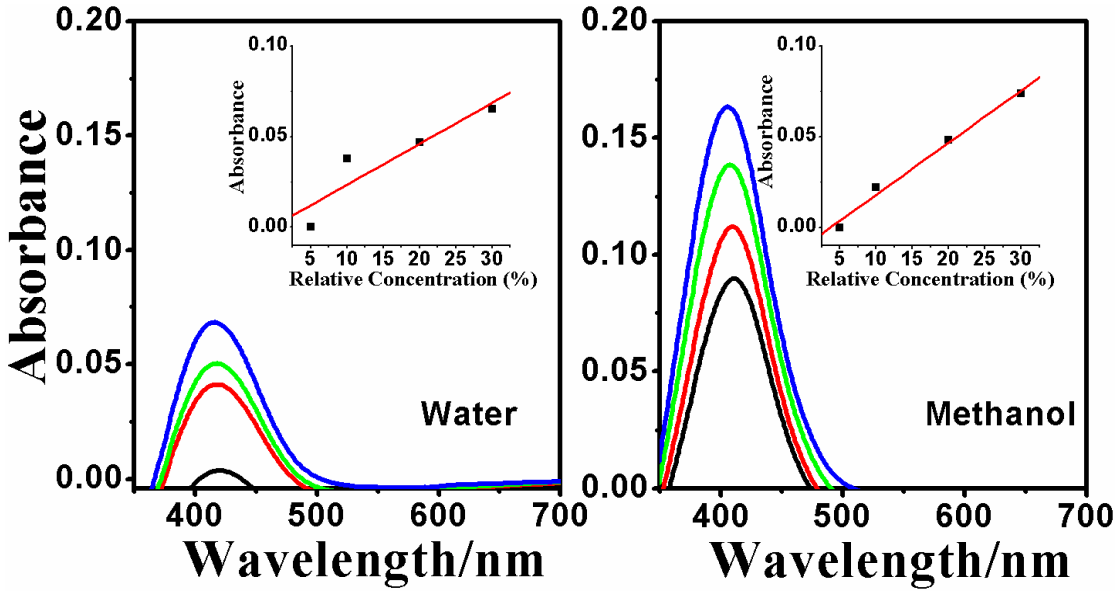

Figure 2.35. UV-Vis absorption spectra of increasing concentrations of AgNPs made by using formaldehyde and 3-APTMS in water and methanol; Respective insets show the dependence of absorption maxima (λ_{max}) on AgNPs concentration.

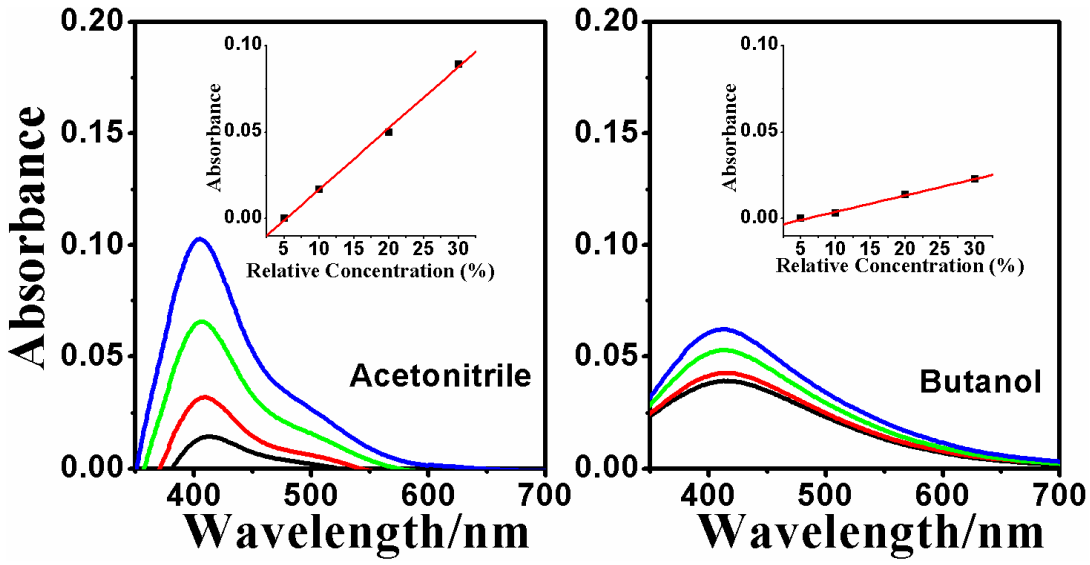

Figure 2.36. UV-Vis absorption spectra of increasing concentrations of AgNPs made by using formaldehyde and 3-APTMS in acetonitrile and butanol; Respective insets show the dependence of absorption maxima (λ_{max}) on AgNPs concentration.

2.4. DISCUSSION

2.4.1. Chemistry of Functionalized Alkoxysilanes Mediated Synthesis of AgNPs

It is necessary, at first instance, to understand the need of two functional alkoxysilanes during the synthesis of AgNPs and to investigate the difference in the dynamics of nanoparticle synthesis as described earlier for AuNPs synthesis [Pandey *et al*., (2014a)]. The synthesis of AuNPs utilizing active role of amines as capping and reducing agent containing trimethoxysilane moiety, has been reported by [Zhu *et al*., (2005)]. They used 3-(trimethoxysilylpropyl) diethylenetriamine (TMSP diene) for AuNPs synthesis and found that the ratio of TMSP/Au^{3+} control the nanogeometry of resulting AuNPs. Time required for AuNPs formation varied from 2 hrs to 23 hrs depending on the ratio of TMSP/Au^{3+}. The unique structure of the TMSP dien–gold complex has shown key point to the rapid auto-reduction. They also observed very slow conversion to nanoparticles when TMSP is replaced with 3-APTMS since prolonged autoreduction tenure enable the hydrolysis and polycondensation of silanol residue. These findings reveal that reducing and stabilizing ability of 3-APTMS however predict the essential requirement of additional reducing agent for real time and controlled nanoparticle synthesis. Accordingly the need of GPTMS, as evidenced

from our previous findings, justifying the reduction of palladium chloride [Pandey *et al*., (2001c); Pandey *et al*., (2003c)] is sought along with 3-APTMS for the conversion of Ag^+ into AgNPs. Further, in order to have deeper insight, the mechanistic role of 3-APTMS and GPTMS mediated synthesis of AgNPs needs to be precisely evaluated. 3-APTMS and GPTMS are hydrophilic and hydrophobic in nature respectively. It is found that GPTMS on mixing with water generates two separate layers whereas a homogeneous single layer is observed in methanolic medium as shown in Figure 2.37. In this process methanol is acting as a reactant converting hydrophobic GPTMS to hydrophilic methanolic solution. The addition of 3-APTMS to GPTMS and vice versa, drastically affects the interaction dynamics which has been one of the findings of the present investigation.

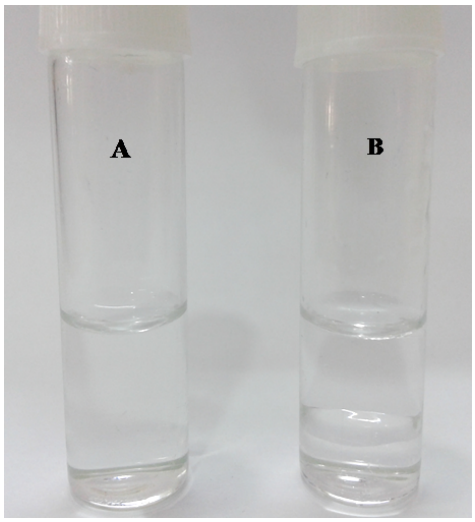

Figure 2.37. Images of methanolic and aqueous suspension of GPTMS. Methanolic suspension of GPTMS (A) shows single layer formed while aqueous suspension of GPTMS (B) results two separate layers.

The results based on these lines reveal significant role of Ag^+ and clearly demonstrate the followings; (1) the addition of GPTMS to 3-APTMS present in reaction system enable faster interaction between glymo- and amino-residue as compared to that of 3-APTMS to GPTMS, justifying the requirement of necessary APTMS molecules per GPTMS molecule (2) addition of 3-APTMS to $AgNO_3$ treated GPTMS allow the slow interaction as justified from relatively small variations in absorbance at 280 nm [Figure. 2.3.] as compared to that of the same when GPTMS is added to 3-APTMS treated silver ion [Figure 2.4.], again justifying the role of

available number of 3-APTMS molecules per GPTMS at the site of glymo-and amino-residue interaction and doesn't enable the synthesis of AgNPs [inset to Figure 2.3.], (3) when GPTMS is added to 3-APTMS in the presence of $AgNO_3$, the new absorbance peak at 280 nm and 420 nm is more facilitated than that of the same without $AgNO_3$, validating that Ag^+ is catalyzing the reaction between glymo- and amino-residues and enable the synthesis of AgNPs [inset to Figure 2.4]. The findings discussed above provided valuable information related to the synthesis of AgNPs and confirmed that only 3-APTMS capped Ag^+ undergo GPTMS mediated reduction of AgNPs. It is again necessary here to understand the reactivity of functional constituents to study the mechanism of such process. The investigation on the specific interaction of 3-APTMS and [2-(3, 4-Epoxycyclohexyl) ethyl] trimethoxysilane resulted into the formation of soild-state network of organically modified silicate thin film [Pandey *et al*., (1999)d; Pandey *et al*., (1999)c]. These observations also predict that 3-APTMS may facilitate the reducing ability of 3-APTMS compatible reducing agent which is a key point during GPTMS mediated synthesis of metal nanoparticles. The epoxide linkage of GPTMS may open in the presence of methanol as evidence from the homogeneous layer in water after the addition of methanol and such epoxide ring opening leads to hydroxy and methoxy derivatives of the same. The interaction of 3-APTMS with metal ions due to their lewis acid character also justifies the reducing ability of 3-APTMS. A mechanism of GPTMS mediated synthesis of AgNPs in the presence of 3-APTMS is hypothesized. The proposed mechanism of 3-APTMS and GPTMS mediated synthesis of AgNPs based on the above observations is shown in Scheme 2.1.

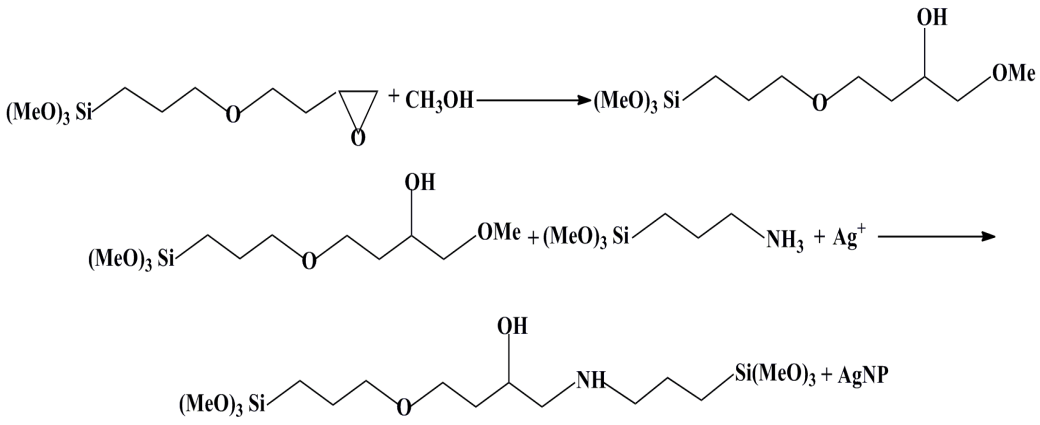

Scheme 2.1. Mechanism of GPTMS and 3-APTMS assisted formation of AgNPs.

The mechanistic approach on the interaction of 3-APTMS and GPTMS may be better explained from the report on the formation of inorganic-organic hybrid [Wight *et al.*, (2002); Utting *et al.*, (2000)]. The role of nitrogen containing compound as base catalyst has been demonstrated and reviewed. It has been shown that 3-APTMS interact with small organic molecule containing aldehyde group, forming imine linkage whereas GPTMS undergo interaction with nitrogen containing organic molecule like imidazole/1, 5, 7-triazabicyclo [4.4.0] dec-5-ene (TBD), forming tertiary amine derivative of glymo-residue. When small organic molecule is replaced by another alkoxysilane (GPTMS/3-APTMS) and allowed the interaction of the same, out of which the first one is hydrophobic whereas the second one being hydrophilic controlled interaction, is recorded. The results recorded in Figure 2.1 and 2.4 reveal that when 3-APTMS is added in excess of GPTMS (Figure 2.1), there has been negligible extent of interaction between two functional alkoxysilanes due to partial homogeneity of the reacting system whereas when GPTMS is added in controlled way into excess of 3-APTMS (Figure 2.1), homogeneity in the system is availed that allowed the interaction of the same since 3-APTMS behaves as a micelle. In addition to that, such functional interaction is facilitated in the presence of Ag^+ resulting into the formation of AgNPs during such process and justifies the originality of the reported process. Such findings further reveal that 3-APTMS treated metal ions move close to methoxy derivative of GPTMS resulting into the formation of amine derivative through NH-group [Pandey *et al.*, (2014a)]. In absence of either 3-APTMS or GPTMS, the synthesis of metal nanoparticles is not observed.

Accordingly, a comparative study was made on the conversion of silver ions and gold ions into AgNPs and AuNPs respectively in the presence of 3-APTMS and GPTMS and to resolve the differences in nanoparticles formation. The findings reported earlier [Pandey *et al.*, (2014a)] clearly demonstrated two important steps recorded during 3-APTMS and GPTMS mediated synthesis of nanoparticles; (1) Interaction of noble metal ions with 3-APTMS and (2) Interaction of 3-APTMS capped noble metal ions with GPTMS. The results as shown in Figure 2.6 justify that the faster interaction of 3-APTMS with gold ions whereas the same is slow with silver

ions (Figure 2.7). Further the GPTMS undergo faster interaction with 3-APTMS capped silver ions (Figure 2.9) whereas the same is slow in case of gold ions (Figure 2.8) under similar conditions. In addition to that the interaction of palladium ions with 3-APTMS and GPTMS is quite different since palladium ions specifically react with glymo-residue of GPTMS followed by reduction of the same together the formation of Pd-C linkage in absence of 3-APTMS as reported earlier [Pandey *et al*., (2001c); Pandey *et al*., (2003c)].

2.4.1.1. Structural Characterization

3-APTMS not only promote such interaction but act as a potent stabilizing reagent for the resulting nanoparticles and the concentration of the same control the dynamics of metal ion and GPTMS reduction, resulting into variable nanogeometry along with suitable control of hydrophilic/hydrophobic components of the NPs. The role of 3-APTMS and GPTMS in controlling the nanogeometry has been evaluated from the data on TEM of AgNPs made at two different cases; (1) variation in 3-APTMS concentrations keeping constant concentration of GPTMS and (2) variation in GPTMS concentrations keeping constant concentration of 3-APTMS. These findings demonstrate the role of functional alkoxysilanes controlling the size of AgNPs and validate the novelty of the present process. The results on the role of amino and glycidoxy-functionalized alkoxysilanes justify the following; (i) behave as active reagents controlling the process of nanoparticle synthesis and (ii) control the nanogeometry of nanoparticles as a function of 3-APTMS/GPTMS concentrations. The formation of AgNPs has also been recorded even at higher concentrations of 3-APTMS (i.e., 3 M) however the results as shown in Table 2.1 justify that the rate of AgNPs formation is faster on increasing GPTMS concentration whereas the same tend to become slow on increasing 3-APTMS concentrations. An increase in 3-APTMS concentrations is normally followed by an increase in viscosity of the medium around metal ions enabling slower interaction with GPTMS required to form AgNPs.

2.4.1.2. Role of 3-APTMS and GPTMS on the Dispersibility of AgNPs in Aqueous and Non-Aqueous Medium

It has been found that the as synthesized AgNPs dispersible in various solvents like aqueous and non-aqueous medium. The two different sizes of AgNPs viz., $AgNP_1$ and $AgNP_3$ are dispersible in four different solvents like methanol, butanol, acetonitrile and dichloromethane. These solvents are of different refractive index. As the particles size increases of the AgNPs, the UV-Vis spectra shifts towards longer wavelengths [Kundu *et al*., (2009); Dong *et al*., (2009); Parmelle *et al*., (2014)] as shown in Figure 2.14-15. Further the observations based on UV-Vis spectroscopy and photography of as synthesized AgNPs (Figure 2.16-21) justifies the dispersibility in two different solvents, having polarity of extreme ends; water and toluene. The data as shown in Tables 2.6–8 justify that AgNPs shows relatively better dispersibility in water when there is an increase in molar ratio of GPTMS to 3-APTMS while decrease in molar ratio of GPTMS to 3-APTMS leads better dispersibility in toluene. Such findings predict that the molar ratio of 3-APTMS to GPTMS is a critical factor affecting the dispersion efficiency of as synthesized AgNPs in aqueous and non-aqueous phase. The higher molar ratio is found to be the optimum under which the dispersion efficiency is better in organic solvent due to increase in the hydrophobic alkyl chain of the reaction product of GPTMS and 3-APTMS. Similarly the lower molar ratio is found to be better for water dispersibility due to relatively less amount of hydrophobic alkyl chain residue (Scheme 2.1).

In order to have deeper insight on the dispersibility of as synthesized AgNPs as a function of their concentrations in butanol, methanol, toluene, dichloromethane and acetonitrile has also been studied. Figures 2.38.(i)–(v) shows linear relation of absorbance as a function of AgNPs concentrations in these solvents with significant variation in λ_{max} as a function of the nature of solvents. There is dependence of λ_{max} on the refractive index of these solvents also, as shown in Figure 2.39. These findings justify potential applications of the AgNPs in a variety of polar and non-polar medium.

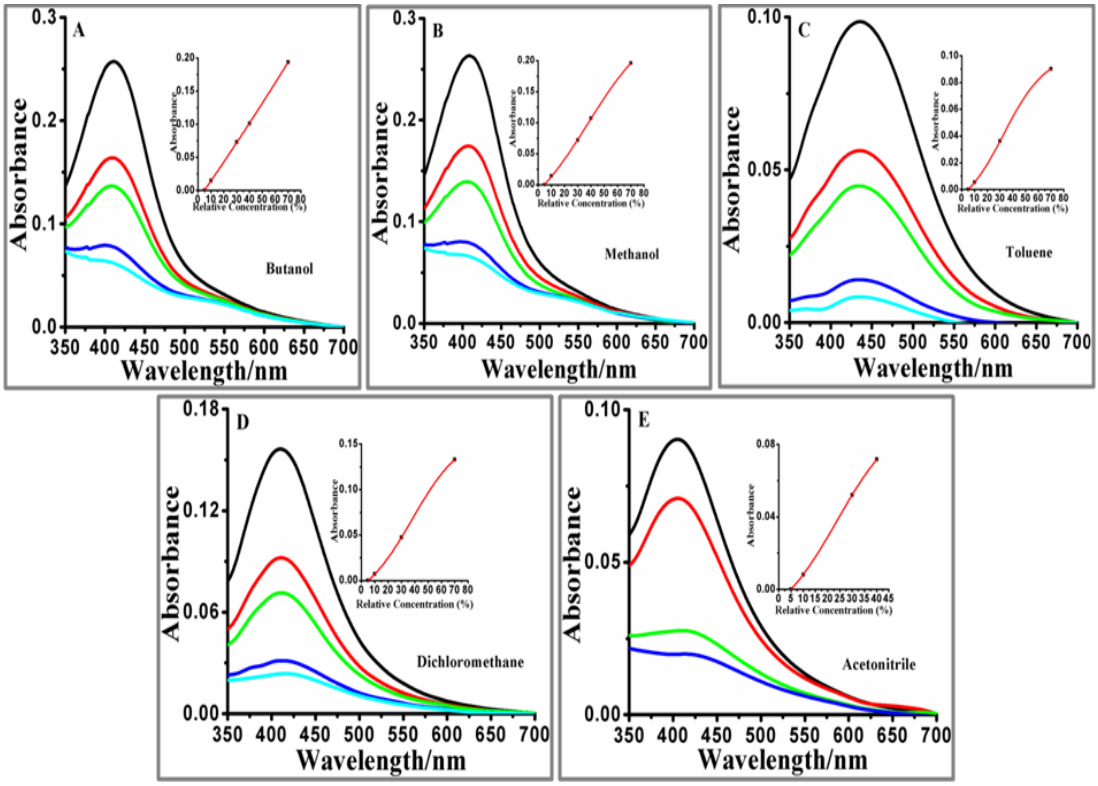

Figure 2.38. UV-Vis spectra of increasing concentrations of AgNP in (A) butanol, (B) methanol, (C) toluene, (D) dichloromethane and (E) acetonitrile. Respective insets show the dependence of absorption maxima (λ_{max}) on relative concentration.

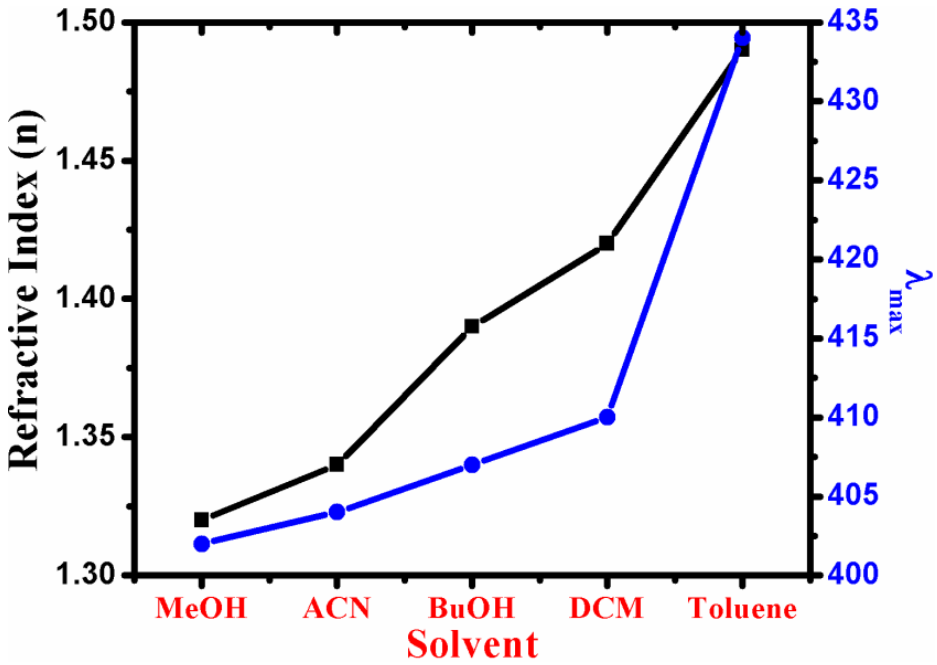

Figure 2.39. Recording shows the dependence of absorption maxima (λ_{max}) on refractive index of solvents.

2.4.2. Synthesis of AgNPs involving the active role of 3-APTMS and Formaldehyde/Cyclohexanone

2.4.2.1 Role of organic reducing agents during 3-APTMS mediated synthesis of AgNPs

At first instant it is important to understand the significance of 3-APTMS during the synthesis of NMNPs. Four major roles of 3-APTMS have been extensively studied for specific applications i.e.; (1) as a potential stabilizer for noble metal nanoparticles [Cushing *et al*., (2004); Daniel and Astruc., (2004); Cango *et al*., (2013); Chaudhari and Paria., (2012)] (2) formation of organic inorganic hybrid as catalytic material [Wight and Davis., (2002)] (3) in the commercial preparation of amino-silanized glass beads/surface functionalized agent having potentiality for Schiff-base linkage/carbodiimide coupling during biotechnological designs [Tewari *et al*., (1995); Weetall., (1993); Woong and Boonton., (1997)] and (4) formation of mesoporous/nanoporous thin film of organically modified silicate [Pandey *et al*., (1999a); Pandey *et al*., (1999b); Pandey *et al*., (1999c); Pandey *et al*., (2003c); Pandey and Singh., (2008); Pandey *et al*., (2001b); Pandey *et al*., (2003a); Pandey and Prakash., (2014d)]. These properties of 3-APTMS directed us to examine its role in nanomaterial synthesis [Pandey and Chauhan., (2012); Pandey *et al*., (2014a); Pandey and Pandey., (2014c)]. We have reported 3-APTMS and GPTMS mediated synthesis of silver nanoparticles (AgNPs) which are dispersible in aqueous media under specific composition of 3-APTMS/GPTMS ratio whereas the same is dispersible in non-aqueous media at all composition. Such findings although, provided a novel report on the synthesis of biocompatible AgNPs, but suffers a disadvantage due to increased alkoxysilane content which limits its use for many practical applications due to the formation of Si–O–Si linkage with time. Accordingly we tried to decrease the silane content by substituting some other reagent in place of GPTMS. Recent reports demonstrated that the 3-APTMS itself does not enable the conversion of noble metal cations (Au^{3+}, Ag^{+} , Pd^{2+}) into respective nanoparticles, however, in the presence of suitable organic reducing agents facilitate the synthesis of the same [Pandey *et al*., (2014b); Pandey and Pandey., (2014c)]. Micellar nature of 3-APTMS enable

controlled synthesis of NPs dispersible in various solvents as a function of organic reducing agents [Pandey *et al*., (2014a)].

The role of 3-APTMS and cyclohexanone has not been limited to noble metal NPs synthesis but also precisely enabled the synthesis of polycrystalline Prussian blue nanoparticles [Pandey and Pandey., (2013a)], revealing the potentiality of these NPs in the formation of nanocomposite. The results, as shown in Figure 2.24-25, clearly demonstrate the rapid synthesis of AgNPs as a function of 3-APTMS concentration in the presence of formaldehyde. The higher concentration of 3-APTMS enable the complete conversion of Ag^+ into AgNPs within < 0.5 h (Figure 2.25) whereas, > 1 h is required at lower 3-APTMS concentration (0.5 M) (Figure 2.24). Exchange of formaldehyde by cyclohexanone under similar condition again causes an increase in time of complete conversion of Ag^+ into AgNPs i.e. 1.5-3 h. In order to understand precisely the requirement of both 3-APTMS and organic reducing agents, the results reveal that the requirement of an optimum concentration of formaldehyde/cyclohexanone for NPs synthesis (in section 2.2.2.3). On the other hand higher concentrations of 3-APTMS always facilitate the AgNPs formation whereas, relatively lower concentration (<0.05M) retard the same. The proposed mechanism for the 3-APTMS and cyclohexanone mediated synthesis is shown in Scheme 2.2:

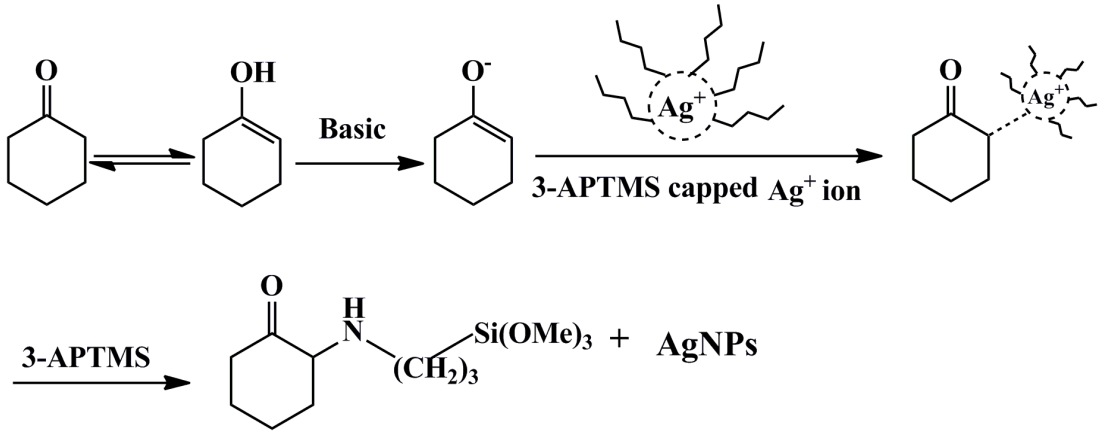

Scheme 2.2. Mechanism of Cyclohexanone and 3-APTMS assisted formation of AgNPs.

Cyclohexanone in the prevailing medium undergoes keto– enol tautomerism. Enolate ion acts as an electron donor to 3-APTMS capped Ag^+ ion, which in turn acts as a Lewis acid, leading to the formation of AgNPs along with organic-inorganic hybrid (Scheme 2.2) and has been confirmed by FTIR spectroscopy (Figure 2.28). The broad band between 3800 and 2800 cm^{-1} is related to the overlap of O-H vibration modes with the organic modes. The IR peaks at 1090-1120 cm^{-1} due to the vibrations of the C-Si-O group. A series of bands at around 2820-2940 cm^{-1} due to the vibrations of methylene -$(CH_2)_3$- and the peaks at about 1220-1275 cm^{-1} are due to the vibrations of Si-CH_3 [Fan *et al*., (2012); Quang *et al*., (2011); Gaspera *et al*., (2011); Duhan *et al*., (2010)]. 3-APTMS and organic reducing agents control the nanogeometry of AgNPs. The TEM images of AgNPs made from cyclohexanone and two different concentrations of 3-APTMS shows circular nanogeometry (Figure 2.29-30) while in presence of formaldehyde and 3-APTMS results in homogeneous dispersion of AgNPs and having higher nanogeometry (Figure 2.32) in comparison to AgNPs made by cyclohexanone and 3-APTMS.

2.4.2.2 Effect of organic reducing agents on the dispersibility of AgNPs

The micellar behaviour of 3-APTMS and the critical micellar concentration of organic reducing agents (cyclohexanone, formaldehyde) play important role in determining the dispersibility of as synthesized nanoparticles. Dispersibility of AgNPs largely depends on the medium which in turn is determined by hydrophilic/hydrophobic behaviour of the organic moieties (formaldehyde/cyclohexanone). The results on the dispersibility of AgNPs, made from 3-APTMS and cyclohexanone in water, methanol, acetonitrile toluene and dichloromethane has been recorded in Figure 2.32-34 facilitate the dispersibility in non-aqueous media whereas, the dispersibility of AgNPs made through 3-APTMS and formaldehyde as a function of their concentrations, (Figure 2.35-36) revealing linear relation between λ_{max} vs AgNPs concentrations

2.5. CONCLUSIONS

First report on the synthesis of functional and processable AgNPs involving the role of 3-APTMS and GPTMS is reported herein. The synthesis of AgNPS

involving active role of 3-APTMS and GPTMS that leads to the formation of AgNPs of average size; 4.7, 7.7 and 8.9 nm is reported. The rate of AgNPs formation is faster on increasing GPTMS concentration whereas the similar increase in rate is observed on decreasing 3-APTMS concentrations. The resulting AgNPs are dispersible in both aqueous and non-aqueous solvents based on the molar ratio of 3-APTMS and GPTMS. An increase in molar ratio of GPTMS to 3-APTMS results better dispersibility of AgNPs in water while decrease in molar ratio of GPTMS to 3-APTMS lead better dispersibility in toluene. The absorption maxima of the AgNPs are found as a function of refractive index of the various organic solvents.

Introduction of Autohydrolysis, condensation and polycondensation during the synthesis of AgNPs directed us to replace one of the alkoxysilane by cyclohexanone / formaldehyde. Accordingly, the second protocol relates to the role of cyclohexanone on the conversion of 3-APTMS capped Ag^+ into AgNPs. Finally, the use of more hydrophilic reducing agent as compared to that of cyclohexanone has been attempted to control the dispersibility of as made AgNPs for practical applications under present condition. Accordingly the role of formaldehyde on the conversion of 3-APTMS capped Ag^+ into AgNPs is described. Their dispersibility in variety of solvents and also enable the formation of organic- inorganic hybrid that facilitated catalytic activity of the same. The finding also demonstrates the requirement of suitable composition of nanoparticles that can be tuned for nanocomposite formation for better catalytic activity with wider applications in both homogeneous and heterogeneous catalysis.